Effects of obesity on the transcriptional regulation of protein degradation in skeletal muscle

by

Lance M. Bollinger

November, 2013

Director of Thesis/Dissertation: Jeffrey J. Brault

Major Department: Kinesiology

Protein degradation is a major cause of skeletal muscle atrophy and is, at least in part, regulated at the level of gene transcription. While obesity is characterized by impaired skeletal muscle carbohydrate and lipid metabolism, the effects of obesity on skeletal muscle protein metabolism, specifically protein degradation, have not been thoroughly examined. Despite increased skeletal muscle mass, skeletal muscle of the severely obese overexpresses protein degradation genes, most notably, myostatin, which increases protein degradation by activating the transcription factor SMAD3, a mediator of transforming growth factor-β family signaling. **GOALS:** The aims of the present project were: 1) to determine how obesity affects skeletal muscle protein degradation mediated by the ubiquitin-proteasome system and the autophagic/lysosomal pathway, particularly at the level of gene expression and 2) to determine the role of SMAD3 in regulating gene transcription of *MuRF-1*, a gene involved in degradation of contractile proteins. **METHODS:** In order to accomplish these goals, primary human skeletal muscle (HSkMC) myotubes from lean and severely obese women were subjected to various atrophic stimuli (100nM dexamethasone or starved of serum and amino acids) and analyzed for gene expression and flux through

the major protein degradation pathways. Additionally, MuRF-1 promoter activity and RNA content were measured following co-expression of SMAD3 and FoxO3, a transcription factor known to induce *MuRF-1* gene expression and cause muscle atrophy. **RESULTS:** Myotubes from the obese significantly overexpressed *FoxO3*, had a decreased rate of flux through the autophagic/lysosomal pathway, and increased proteasome capacity compared to lean. Despite these differences, myotubes from lean and obese women atrophied at similar rates and displayed similar total protein degradation rates under basal and starved conditions. Additionally, SMAD3 overexpression was insufficient to induce *MuRF-1* promoter activity or gene expression, but synergistically augmented FoxO3-induced *MuRF-1* gene expression by increasing FoxO3 protein content and enhancing FoxO3 binding to the proximal MuRF-1 promoter region. Furthermore, knockdown of SMAD3, via overexpression of a dominant-negative SMAD3, significantly attenuated FoxO3-induced *MuRF-1* promoter activity. Mutation of the SMAD Binding Element (SBE) within the MuRF-1 promoter region attenuated FoxO3 binding to the FoxO Response Element (FRE), indicating SMAD3 is required for optimal FoxO3-induced *MuRF-1* gene transcription. **CONCLUSIONS:** Skeletal muscle of the severely obese displays altered flux through the major protein degradation pathways, which may contribute to some of the metabolic impairments associated with obesity. However, severe obesity does not affect the total protein degradation rate or rate of muscle atrophy. Furthermore, SMAD3 regulates *MuRF-1* gene transcription through dual mechanisms: 1) increasing FoxO3 protein content and 2) increasing FoxO3 binding within the proximal *MuRF-1* promoter region. Atrophic conditions that increase SMAD3 transcriptional activity may augment FoxO3-induced transcription of protein degradation genes and accelerate muscle atrophy. Due to the observed overexpression

of *FoxO3*, skeletal muscle of the severely obese may be more susceptible than that of lean persons to atrophy under conditions that increase expression and/or activity of SMAD3.

# Effects of obesity on the transcriptional regulation of protein degradation in skeletal muscle

A Dissertation

Presented To the Faculty of the Department of Kinesiology

East Carolina University

In Partial Fulfillment of the Requirements for the Degree

Doctor of Philosophy

by

Lance M. Bollinger

November, 2013

Effects of obesity on the transcriptional regulation of protein degradation in skeletal muscle

by

Lance M. Bollinger

APPROVED BY:

DIRECTOR OF
DISSERTATION/THESIS: _____
(Jeffrey J. Brault, Ph.D.)

COMMITTEE MEMBER: _____
(Joseph A. Houmard, Ph.D.)

COMMITTEE MEMBER: _____
(Robert C. Hickner, Ph.D.)

COMMITTEE MEMBER: _____
(David A. Tulis, Ph.D.)

CHAIR OF THE DEPARTMENT
OF Kinesiology: _____
(Stacey Altman, J.D.)

DEAN OF THE
GRADUATE SCHOOL: _____
Paul J. Gemperline, PhD

ACKNOWLEDGEMENTS

I would like to thank my mentor, Dr. Jeffrey J. Brault for his support throughout my doctoral career. Additionally, I would like to thank Dr. Carol A. Witczak for her intellectual input, technical assistance, and generosity with her laboratory equipment and materials. I would also like to thank Dr. Joseph A. Houmard for providing me with the primary cell cultures used throughout this project and Dr. Jill Maples for her tremendous assistance with the technical aspects of these cultures. I would like to thank the American College of Sports Medicine for their financial support. I would also like to thank my fellow students for their contributions, both intellectual and technical. Special thanks are due to J. Matthew Hinkley, Jonathon J. Powell, Patrick Davis, and Sanghee Park. On a personal level, I would like to thank my family. Thank you to my son, Henry for always brightening my day when I return from work. Finally, I would like to thank my beautiful wife, Emily, for her support, encouragement, and motivation.

LIST OF TABLES

LIST OF FIGURES

LIST OF FIGURES (cont.)

TABLE OF CONTENTS

TABLE OF CONTENTS (cont.)

## Chapter 1: Global introduction and literature review

### Importance of Protein Degradation in Obesity:

Severely decreased skeletal muscle mass, or muscle atrophy, affects over five million American adults, frequently presents secondary to other physiological (aging, fasting, or physical inactivity) or pathological (diabetes, heart failure, renal failure, respiratory disease, or cancer) conditions (68), and is a major cause of disability (47) and death (64, 71, 80, 95). Despite a plethora of negative consequences, obesity is accompanied by increased skeletal muscle mass (27, 69), fiber diameter (28), and strength (53). The molecular mechanism(s) underlying the observed hypertrophic phenotype in obesity is not well understood. Furthermore, obesity exacerbates the negative effects of muscle atrophy; the combination of obesity and muscle atrophy increases risk of death to a greater extent than either condition independently (80). However, it is not known whether obesity *per se* increases the risk of developing muscle atrophy.

Myocellular size, and therefore, skeletal muscle mass is dictated by the balance between the rates of protein synthesis and degradation (34). Interestingly, the protein synthesis response to muscle atrophy is highly variable. While many cachectic conditions are associated with decreased protein synthesis rates, it has previously been demonstrated that immobilization-induced atrophy occurs despite no change in protein synthesis rates (51). However, protein degradation rate increases in all known models of muscle atrophy (13, 54, 82). Obese mice (92), rats (74), and humans (23, 75) have a blunted hypertrophic response to muscle overload and feeding (27). Therefore, it is

unlikely that the increased skeletal muscle mass observed in obesity is due to an increased rate of protein synthesis.

The effects of obesity on protein degradation are poorly understood and remain controversial (48). During fasting, the typical increase in proteolysis is blunted in obese humans (27, 73). In contrast to these findings, Felig et al. (24) noted increased proteolysis in obesity as indicated by elevated plasma amino acids following an overnight fast. Protein degradation at the whole-body level has been shown to be increased in obesity (39, 103). Furthermore, diet-induced obesity increases expression of genes involved in protein degradation such as myostatin (42, 72). Due to these discrepant findings, the effects of obesity on skeletal muscle protein degradation remain controversial.

Protein degradation is mediated primarily by two pathways, the ubiquitin-proteasome system (UPS) and the autophagic/lysosomal pathway (11, 107), and is essential for proper cellular function due to its role in eliminating damaged, misfolded or non-functional proteins and protein aggregates (66). Accelerated protein degradation is a major cause of muscle atrophy (65).

While the mechanisms controlling protein degradation are complex, it appears that numerous cachectic conditions share a common transcriptional response to increase protein degradation (13, 54, 82). Using RNA microarray analysis, Lecker et al. (54) identified over 700 genes that were coordinately up- or down-regulated in at least two cachectic conditions and 133 that were coordinately regulated in four. Interestingly, the transcriptional response to increase protein degradation appears to be largely driven

by only a few transcription factors, most notably FoxO (83, 93, 107) and SMAD3 (13, 35, 56, 85). Unfortunately, the cellular mechanisms that transcriptionally regulate flux through the major protein degradation pathways are incompletely understood, especially in obesity.

## Protein Degradation Pathways

Protein degradation is mediated primarily by two pathways with functionally distinct roles: the ubiquitin-proteasome system (UPS) and the autophagic/lysosomal pathway (84). Together, these systems account for greater than 90% of protein degradation in mammalian cells and flux through both pathways is increased during muscle atrophy (11, 107).

The ubiquitin-proteasome system (UPS) selectively degrades proteins in an ATP-dependent manner (22, 70) and accounts for approximately 70% of total protein degradation in mammals (46). The UPS consists of a multitude of highly regulated proteins that selectively tag and degrade damaged, misfolded, or unnecessary proteins (40, 104). Ubiquitin ligases selectively attach polyubiquitin chains to target proteins which are recognized by the 19S cap of the proteasome. Proteins are then unfolded and degraded by the 20S proteasome and constitutive amino acids and ubiquitin are recycled. Flux through the UPS is dependent on protein ubiquitination as well as proteasome subunit composition and binding partners that alter catalytic activity of the proteasome (21, 76).

UPS-mediated protein degradation is regulated, at least in part, by gene transcription. Gene expression of two muscle-specific ubiquitin ligases, Muscle-Specific RING Finger-1 (*MuRF-1)* and *Atrogin-1*, increases dramatically during muscle atrophy (54, 82). These ubiquitin ligases have functionally distinct roles, but both are essential for muscle atrophy (8). MuRF-1 functions primarily to target proteins of the thick filament for proteasome-mediated protein degradation (17, 18). Atrogin-1 promotes degradation of eukaryotic translation initiation factor 3F (eIF3-F) (20), desmin and vimentin (58). Additionally, Atrogin-1 putatively interacts with sarcomeric proteins (58). Transcription of *Atrogin-1* and *MuRF-1* is largely dependent on the transcription factor Forkhead box "O" (FoxO) (83, 93, 100). During muscle atrophy, activating the PI3K/Akt pathway with IGF-1 results in a marked phosphorylation and cytosolic sequestration of FoxO1 and FoxO3, prevents upregulation of ubiquitin ligases, and preserves myocellular size (93). Interestingly, MuRF-1 protein is higher in skeletal muscle of the obese (91), suggesting flux through this pathway may be disrupted in obesity.

Like the UPS, the autophagic/lysosomal pathway is a major contributor to protein degradation (84). It has recently been reported that, compared to the UPS, the autophagic/lysosomal pathway is upregulated to a greater extent during muscle atrophy (11, 107). While the autophagic/lysosomal pathway can selectively degrade specific individual proteins, one major role of this pathway is degradation of organelles such as mitochondria (32). Autophagosomes, double membraned vesicles form within the cell, recognize and engulf cellular material labeled for degradation. Autophagosomes fuse with lysosomes to form autophagolysosomes and hydrolases contained within the lysosome non-selectively degrade proteins and organelles contained within the vesicle.

Impaired flux through the autophagic/lysosomal pathway has been shown to result in accumulation of damaged mitochondria and cause insulin resistance (106). Therefore, it is possible that impaired autophagic/lysosomal flux may contribute to some of the metabolic perturbations associated with obesity.

Importantly, the autophagic/lysosomal pathway, like the UPS, appears to be transcriptionally regulated. Microtubule-associated protein 1 light chain 3β (LC3) associates with the inner membrane of autophagosomes and proteins labeled for degradation, thus committing these proteins to the autophagosome. Due to its location within the autophagosome, LC3 is degraded by lysosome hydrolases within the autophagolysosome. Therefore, transcription of LC3 must increase in order to replenish that consumed during protein degradation (98). Therefore, in order to sustain autophagic/lysosomal-mediated protein degradation, transcription of LC3 must be increased. Recently, Zhao et al. (107) demonstrated that FoxO3 overexpression increases gene expression of LC3, Gabarapl-1, and Atg12 in muscle cells.

**Transcription factors regulating protein degradation**

Forkhead box type "O" (FoxO) coordinately regulates both UPS and autophagic/lysosomal-mediated protein degradation by increasing transcription of genes essential to these pathways. Knockdown of FoxO (81, 87) is sufficient to preserve muscle mass during atrophic conditions indicating that FoxO-induced gene transcription is essential for increased protein degradation. FoxO transcription factors recognize the consensus FoxO Response Element (FRE) (A/G)TAAA(T/C)A within the promoter

region to induce gene transcription (31, 83, 107). Transcriptional activity of FoxO is inhibited by Akt-mediated phosphorylation and subsequent cytosolic sequestration (93). Insulin resistance, a common side-effect of severe obesity (77), decreases Akt activity and may thus increase FoxO-induced gene transcription and protein degradation.

Despite its ability to induce muscle atrophy, FoxO alone may be insufficient to fully activate gene transcription. Waddel et al. (100) recently demonstrated that the glucocorticoid receptor synergistically increases FoxO-induced transcription of MuRF-1. Furthermore, the close proximity of the glucocorticoid response element and the FRE within the MuRF-1 promoter region suggests that FoxO may form transcriptional complexes with complementary DNA-binding factors to augment FoxO-induced gene transcription. In support of this, Ramaswamy et al. (79) demonstrated that a FoxO mutant lacking the DNA binding domain maintained the ability to induce gene transcription.

SMAD3, a transcription factor that mediates Transforming Growth Factor-β (TGF-β) family signaling, is a major determinant of protein degradation and plays a central role in the development of muscle atrophy (13). SMAD3 is phosphorylated (activated) by ligand-receptor binding and associates with SMAD4 to gain nuclear access (61). SMAD3 directly interacts with DNA at the SMAD binding element (SBE, AGAC) to induce gene transcription (90). While SMAD3 regulates gene expression of numerous genes, SMAD3-induced gene transcription is often relatively weak and non-specific unless accompanied by a complementary transcription factor (61). Myostatin, a TGF-β family member, is elevated in numerous atrophic conditions such as heart failure,

glucocorticoid treatment, disuse, and cancer cachexia (14, 19, 29, 38, 55, 60, 102) and increases protein degradation in a SMAD3-dependent manner (56). Overexpression of SMAD3 alone is sufficient to induce *Atrogin-1* gene expression, increase protein degradation rate, and cause muscle atrophy (35, 85). Interestingly, myostatin expression (1, 42, 59, 72) and SMAD3 activity (101) are increased in skeletal muscle of the severely obese, suggesting skeletal muscle of the obese may be more susceptible to muscle atrophy

To date, the combined effects of FoxO and SMAD3 on protein degradation and muscle atrophy have not been explored. These transcription factors are known to directly interact (88) and coordinately regulate gene expression (2, 33, 88). Therefore, it is possible that FoxO3 and SMAD3 coordinately increase transcription of protein degradation genes during muscle atrophy.

## Conclusions

Obesity is accompanied by both increased skeletal muscle mass and overexpression of genes involved in protein degradation. Increased expression of protein degradation genes may put obese persons at increased risk of muscle atrophy during cachectic conditions such as heart failure, cancer, and type 2 diabetes. To date, the effects of obesity on muscle mass and protein degradation have largely been ignored and the studies that have been performed have yielded conflicting results. A common transcriptional response to muscle atrophy increases both UPS and autophagic/lysosomal-mediated protein degradation which is driven, in large part, by the transcription factor FoxO. Decreased Akt activity in obesity-induced insulin resistance

may increase FoxO-induced gene transcription. Additionally, increased TGF-β signaling, which is commonly observed in skeletal muscle of the obese, may augment FoxO-induced gene transcription and exacerbate muscle atrophy. Therefore, the present project aimed to define the effects of obesity on the transcriptional regulation of skeletal muscle protein degradation. Specifically, we hypothesized that:

1) Skeletal muscle of the obese overexpresses genes involved in the major protein degradation pathways.
2) Protein degradation rate and flux through the major degradation pathways is higher in skeletal muscle of the obese.
3) Skeletal muscle of the obese is more susceptible to muscle atrophy.
4) SMAD3 augments FoxO-induced transcription of ubiquitin ligases.
5) SMAD3 increases FoxO binding to the FRE within the promoter region of FoxO-inducible gene *MuRF-1*.

# Chapter 2: Myotubes from lean and severely obese women degrade proteins at similar rates despite altered ubiquitin-proteasome system and autophagic/lysosomal pathway flux


## Abstract:

Obesity is commonly accompanied by increased skeletal muscle mass, yet this tissue overexpresses many genes involved in protein degradation. Despite evidence of increased whole-body protein turnover, the effects of obesity on skeletal muscle protein degradation have not been systematically explored. The purpose of the present project was to determine how obesity affects protein degradation and transcription of atrophy-related genes. **Methods:** Primary Human Skeletal Muscle (HSkMC) myotubes, a cell culture model that retains many characteristics of obesity, from 10 lean and 8 severely obese women were subjected to both hypertrophic (IGF-1) and atrophic (dexamethasone or serum and amino acid starvation) stimuli. Gene expression patterns (RT-PCR), protein degradation rate, proteasome activity, and myotube area were measured at 24 h. **Results:** Gene expression patterns were similar between myotubes of lean and severely obese individuals with the exception of the transcription factor *FoxO3,* which was significantly higher in the severely obese. Total protein degradation rate was similar between myotubes of the lean and severely obese. However, the rate of flux through the autophagic/lysosomal pathway was slower in myotubes from the obese. Additionally, during starvation, the rate of flux through the ubiquitin-proteasome system (UPS) decreased in myotubes of the lean, but increased in myotubes of the obese, indicating a shift toward UPS-mediated protein degradation.

Furthermore, myotubes from the obese displayed elevated proteasome activity. Despite altered flux through the major protein degradation pathways, myotube area was similar between lean and obese under basal and starved conditions. **Conclusions:** Despite increased gene expression of FoxO3, obesity does not affect the overall rate of muscle protein degradation but does alter flux through the major protein degradation pathways. Since the UPS and autophagic/lysosomal pathway preferentially degrade different cellular proteins and protein complexes, these findings suggest that the turnover rate of specific proteins may differ between lean and obese.

## Introduction

Obesity affects over one-third of American adults (25) and is a major risk factor for other chronic diseases and premature mortality (26). Deficiencies in skeletal muscle carbohydrate and lipid metabolism underlie many of the metabolic abnormalities associated with obesity, such as type 2 diabetes (36). Furthermore, even though skeletal muscle mass is commonly increased in obese individuals (27, 69), skeletal muscle protein metabolism may also be impaired (48). However, this has not been thoroughly examined and remains controversial (48). Protein degradation is essential to proper cellular function. Impaired protein degradation results in accumulation of misfolded, damaged, or otherwise non-functional proteins (66). Alternatively, accelerated protein degradation is a major cause of muscle atrophy (65), which increases risk of disability and death (80).

Protein degradation is mediated primarily by two pathways, the ubiquitin-proteasome system (UPS) and the autophagic/lysosomal pathway. The UPS accounts for the majority of basal cellular protein degradation (46). Ubiquitin ligases target specific proteins for UPS-mediated degradation via polyubiquitination. Flux through the UPS is dictated by proteasome assembly and activity as well as protein polyubiquitination and deubiquitination (76). The autophagic/lysosomal pathway mediates degradation of the bulk of the remainder of cellular proteins, especially macromolecules and organelles such as mitochondria through macroautophagy (84). During this process, autophagosomes engulf cellular components, fuse with lysosomes,

and proteins are degraded by lysosomal hydrolases. It is important to note that both pathways are upregulated during muscle atrophy (107).

Interestingly, a common gene transcription profile has been observed in response to numerous stimuli that increase protein degradation rate (54, 82). The transcription factors Forkhead Box O 1 and 3 (*FoxO1)* and (*FoxO3)* are upregulated in response to numerous atrophic stimuli (54). These transcription factors regulate expression of the ubiquitin ligases *Atrogin-1* and Muscle-specific RING Finger-1 (*MuRF-1*), as well as genes involved in autophagic/lysosomal-mediated protein degradation, such as microtubule-associated protein 1 light chain 3β (*LC3*), GABA(A) receptor-associated protein like-1 (*Gabarapl-1*), and autophagy-related 4B (*ATG4B*) (8, 83, 100, 107). Therefore, FoxO transcription factors appear to be master regulators of muscle atrophy by activating both the UPS and autophagic/lysosomal pathways.

To date, studies regarding protein degradation in obesity have yielded controversial results. Obesity is accompanied by increased strength (53), skeletal muscle mass (27, 69), and increased fiber diameter (28) compared to lean, suggesting the basal rate of protein degradation may be repressed. Further, protein degradation may be less sensitive to atrophy signals, since during fasting the typical increase in proteolysis is blunted in obese humans (27, 73). In contrast, others have noted that basal whole-body rates of protein degradation may be increased in obesity (24, 39, 103), and diet-induced obesity increases expression of genes involved in protein degradation such as myostatin (42, 59, 72) and MuRF-1 (91). Unfortunately, these *in vivo* studies are confounded by muscle overload, nutritional status, and elevated

circulating amino acids, factors that can alter protein metabolism and are inherently different between lean and obese subjects. Therefore, given the prevalence of obesity, the roles of protein degradation in muscle mass regulation and cellular function, and the conflicting body of data regarding protein degradation in obesity, it is important to directly measure muscle protein degradation rates in obesity.

Due to the well-described insulin resistance *in vivo* and *in vitro* (43) and elevated myostatin expression seen in skeletal muscle of the severely obese (1, 42, 72), we hypothesized that expression of protein degradation-related genes and rates of protein degradation would be higher basally in myotubes from the severely obese and that the myotubes from the obese would be more sensitive to signals known to alter protein degradation. To this end, we measured protein degradation and gene expression profiles of cultured primary human skeletal muscle myotubes (HSkMC), a model that retains many characteristics of obesity *in vitro* (6, 10), in response to both hypertrophic and atrophic stimuli.

## Methods

### Human subjects and muscle biopsies.

Lean (BMI 18.5-26.0 kg/m$^2$, n=10) and severely obese (BMI 39.0-57.3 kg/m$^2$, n=8) subjects were recruited through ongoing studies on obesity at East Carolina University. Muscle biopsy procedures were approved by East Carolina University Institutional Review Board and no personal identifiers were retained. Blood samples were collected following an overnight fast and plasma glucose and insulin were measured. Homeostatic model assessment (HOMA-IR), a marker of insulin resistance (62), was calculated (fasting plasma glucose x fasting plasma insulin/22.5). Subject characteristics are presented in Table 2.1.

### Cell culture.

Primary Human Skeletal Muscle (HSkMC) myoblasts were generated as previously described (5) by isolating satellite cells from muscle biopsies of the vastus lateralis of lean and severely obese female subjects. Myoblasts were cultured in Dulbecco's modified Eagle's medium (DMEM, 1g glucose/L) supplemented with 10% fetal bovine serum, recombinant hEGF, dexamethasone, gentamycin, BSA, and fetuin (SkGM Singlequots, Lonza). Upon reaching confluence, growth media was switched to low serum media (2% horse serum) supplemented with 3% BSA and 0.1% fetuin to induce differentiation into myotubes. All experiments were performed on myotubes of

similar passage number (4-5) and days post-differentiation (6-8) to ensure these variables did not affect results.

For experiments using pooled myotubes (UPS flux, autophagic/lysosomal flux, and proteasome capacity), myotubes were cultured individually until 50% confluent then seeded together in multiwell plates, allowed to adhere to the plate overnight, then switched to low serum media to induce differentiation. Myoblasts were cultured independently prior to differentiation to eliminate effects of differing growth rates between myoblast cultures. Pooled data was collected on two independent pools to confirm the accuracy of results.

Myotubes were starved of serum and amino acids (cultured in HBSS) or treated with 100nM dexamethasone to induce protein degradation. Additionally, myotubes were treated with 100nM IGF-1 to inhibit protein degradation. 100nM dexamethasone maximally induces protein degradation of C2C12 and L6 myotubes (63) and 100nM IGF-1 is sufficient to increase protein synthesis in HSkMC (Supporting information 2.1).

**Real-time PCR.**

Total RNA was extracted from myotubes using TRIzol following 24 h of starvation, IGF-1 or dexamethasone treatment. RNA concentration and purity was assessed spectrophometrically (Ab260/280) using a NanoDrop UV-Vis spectrophometer (ThermoScientific, ND-1000). Integrity of RNA was confirmed by agarose gel electrophoresis on a subset of individuals to ensure RNA was not degraded prior to

reverse transcription. RNA was then reverse transcribed (Quanta Biosciences) and RT-PCR performed (SYBR green chemistry, Applied Biosystems 7900HT) using standard methods as previously described (107). The expression of Large Ribosomal Protein (RPLPO), which was not different between lean and obese groups, was used as an endogenous control, and the fold expression of genes of interest was calculated using the relative standard curve method. Standard curves were tested over eight orders of magnitude and amplification efficiency was near 100%. Custom RT-PCR primers (Table 2.2) were generated using NCBI BLAST algorithms (http://blast.ncbi.nlm.nih.gov/Blast.cgi) and specificity confirmed by conventional PCR followed by agarose gel electrophoresis.

**Protein degradation rate.**

Degradation rate of long-lived proteins was determined as previously described (11). Myotubes were radiolabeled with L-[3,5-$^{3}$H] tyrosine (5-10μCi/ml, PerkinElmer Life Sciences) for 24 h. Cells were washed and radioactivity chased for 2 h using differentiation media supplemented with 2mM L-tyrosine to allow degradation of short-lived proteins and to limit re-incorporation of the radiolabel. Fresh media was added, and media samples (3 or 4) were collected over time. As we have previously reported, protein degradation rate (radioactivity release) is curvilinear over the course of 30 h (107). Therefore, we assessed protein degradation over two time periods, either 0-5 h or 20-30 h. The rates over these time periods were highly linear ($R^2$>0.97) for all individuals. At the end of the experiments, culture media was removed completely and myotubes were solubilized in 0.2N NaOH. Radioactivity of cells and TCA-precipitated

media samples was measured using scintillation counting. Total radioactivity was calculated as the sum of the residual radioactivity in the myotubes plus radioactivity of all time points. Protein degradation rate was calculated from the regression line of serial samples for each individual and is given as a percentage of total [$^3$H] tyrosine incorporation.

**Protein content.**

In a parallel experiment, myotubes were treated with IGF-1, dexamethasone, or starved for 24 h and cellular protein was collected. Myotubes were washed twice with PBS and proteins collected with 300µl freshly made Radio-Immunoprecipitation Assay (RIPA) buffer containing 1% NP-40, 0.5% sodium deoxycholate, 0.1% SDS, and protease inhibitor cocktail (Roche Complete Mini). Samples were vortexed continuously for 1min, rotated end-over-end for 30 min, then centrifuged at 12,000 x g for 10min and the pellet discarded. Samples were stored at -80°C until processing and protein concentration (µg/ml) determined by bicinchoninic acid (BCA) assay (ThermoScientific).

**Relative flux through the UPS and autophagy pathways.**

In order to calculate relative flux through the UPS and autophagic/lysosomal pathways, we repeated the protein degradation assay described above in the presence of the highly specific proteasome inhibitor PS-341 (Bortezomib/Velcade) or the highly specific lysosome acidification inhibitor Concanamycin A as previously described (11, 107) using pooled myotubes (3 individuals per pool). During the two hour chase,

myotubes were pre-incubated with 1.0μM PS-341 and/or 0.1μM Concanamycin A for 1 h and these inhibitors remained in the culture media for the duration of the experiment. Relative flux through the UPS and autophagy pathways was determined by subtracting the inhibitor-sensitive degradation rate from the basal degradation rate (Basal degradation rate – degradation rate with inhibitor = degradation rate attributable to inhibited pathway). Differences between lean and obese myotubes were determined by subtracting the lean protein degradation rate from the corresponding value for the obese (Δ Degradation rate = degradation $rate_{obese}$ – degradation $rate_{lean}$)

**Proteasome activity.**

Pooled myotubes (3 individuals per pool) were cultured in serum and amino acid free media for 24 h. Purified proteasomes were collected as described by Kisselev and Goldberg (49). Briefly, cell lysates were collected in buffer containing: 50mM Tris-HCl, pH 7.5, 250mM sucrose, 5mM $MgCl_2$, 2mM ATP, 1mM DTT, 0.5mM EDTA and 0.025% digitonin to permeabilize the cell membrane. Lysates were centrifuged at 20,000 x g for 15 min to isolate the cytosolic fraction (supernatant) and chymotrypsin-like activity of the proteasome analyzed immediately. The cytosolic fractions were plated in black 96 well microplates (30μl per well). The fluorogenic amino acid substrate Suc-LLVY-amc (100μM final concentration, Bachem) was diluted in proteasome activity buffer and added to the microplate wells. This substrate fluoresces upon chymotrypsin-like cleavage by the proteasome. Fluorescence (excitation 380, emission 460) was measured using a microplate reader (Spectromax M4) over the course of 15 min.

Proteasome specificity for Suc-LLVY-amc was confirmed by treating cytosolic extracts with 100μM PS-341 (Bortezomib/Velcade). Results were standardized to total protein content of the cytosolic fraction (DC protein assay, BioRad) to control for differences in proteasome content.

**Myotube area.**

Myotube area was quantified by analyzing the amount of myosin heavy chain covering the culture area (immunofluorescence) and total number of nuclei counted after staining with 4',6-diamidino-2-phenylindole (DAPI). Myoblasts (~40% confluency) were plated in six well plates, grown to confluence, differentiated for 6-7d, and cultured in starvation media (HBSS) for 24 h. Briefly, myotubes were washed with a cytoskeleton stabilizing buffer containing 80mM PIPES, 5mM EGTA, 1mM MgCl2, and 40g/L PEG 35,000 as described by Trendelenurg et al (99). Cross-linking was performed with 4% paraformaldehyde, and myotubes were permeabilized with 0.1% Triton X-100. Non-specific binding was blocked with 10% rat serum. Myotubes were then incubated with an antibody that detects all isoforms of myosin heavy chain (A4.1025, 1:100 dilution, Developmental Studies Hybridoma Bank) overnight at 4ºC. Immunofluorescence was achieved using a fluorogenic secondary antibody (AlexaFluor 546, Invitrogen) and DAPI. Myotubes were then imaged at 10x magnification using a fluorescent microscope (Leica DMI 4000B). Antibody specificity was confirmed by the striated appearance of myotubes. Wells (n=2 per condition) were divided into 10 regions and a single image collected from each region (20 images/condition/individual).

Images were then processed using open-access software from NCBI (Image J, rsbweb.nih.gov/ij/) with a self-designed macro. Images were split from RGB format to individual components (TRITC and DAPI), converted to threshold images, and analyzed for positive pixels (myosin heavy chain) or individual particles (nuclei count). The total myosin heavy chain area was standardized to the number of nuclei to control for differences in seeding density.

**Statistical analysis.**

Statistical analysis for gene expression, protein degradation rate, protein content, and myotubes area data were determined by two-way repeated measures ANOVA with Sidak post-test comparisons. Given our data mean and standard deviations for the protein degradation assay, a power analysis revealed that we would need 6-7 observations to have an 80% chance of achieving a statistically significant difference with $\alpha=0.05$. Data from pooled myotubes (UPS flux, autophagic/lsysomal flux, and proteasome activity) were determined by two-way ANOVA with Sidak post-test comparisons. Statistical analysis was performed using SPSS 19 and significance was set at $\alpha=0.05$.

## Results

### Subject Characteristics

Subjects were classified as lean or severely obese on the basis of body mass index (BMI, kg/m$^2$). By definition, severely obese (≥ 39.0 kg/m$^2$) subjects displayed a higher BMI than their lean counterparts (≤ 26.0 kg/m$^2$). Additionally, the severely obese were significantly older than lean and displayed marked insulin resistance as assessed by homeostatic model assessment (HOMA-IR).

### Differential atrophy-related gene expression between lean and obese myotubes

In order to determine how severe obesity affects the transcriptional response to muscle atrophy, we performed RT-PCR after 24 h of exposure to IGF-1, dexamethasone, or starvation. Due to their roles in protein degradation, we analyzed genes involved in the UPS (*FoxO3*, *Atrogin-1*, and *MuRF-1*) and the autophagic/lysosomal pathway (*LC3B*, *Gabarapl-1*, and *ATG4B*). These genes are known to be, at least in part, transcriptionally regulated (54, 107). Furthermore, due to the well-documented increased myostatin expression (1, 42, 72) and TGF-β signaling in obesity (101), we analyzed genes involved in the myostatin/TGF-β signaling pathway.

As shown in Figure 2.1A, starvation increased gene expression of *MuRF-1* (lean: 3.1 and obese: 4.5 fold) and *Atrogin-1* (lean: 2.3, obese: 2.6 fold). Interestingly, starvation increased *FoxO3* gene expression in myotubes from the severely obese (1.4 fold), but had no effect on myotubes from lean subjects. Dexamethasone treatment

significantly increased gene expression of *MuRF-1* (lean: 2.1 and obese: 2.5 fold) and *FoxO3* (lean: 1.2 and obese: 1.5 fold), but had no effect on *Atrogin-1*. IGF-1 treatment significantly reduced gene expression of *FoxO3* (lean: 0.8 and obese: 0.9 fold), but did not affect *MuRF-1* or *Atrogin-1* gene expression.

Starvation significantly altered expression of genes involved in the autophagic/lysosomal pathway (Figure 2.1B). Specifically, gene expression of *Gabarapl-1*, a gene essential for autophagosome formation, was significantly increased (lean: 1.3 and obese: 1.7 fold) in response to 24 h of starvation. Gene expression of *ATG4B*, another regulator of autophagosome formation, was significantly reduced in response to 24 h of starvation (lean: 0.7 and obese: 0.9 fold). LC3B is essential in committing proteins to the autophagosome membrane for degradation and, due to its location within the autophagosome, is degraded during autophagy (98). Therefore, LC3B transcription must increase in order to sustain flux through the autophagy pathway. Surprisingly, *LC3B* gene expression was unchanged after 24 h of starvation. In contrast to starvation, neither dexamethasone, nor IGF-1 had any effect on *Gabarapl-1*, *ATG4B*, or *LC3B* gene expression.

The TGF-β signaling pathway is known to negatively regulate muscle mass and signaling through this pathway is increased in severe obesity (101). This is especially true for the muscle-specific cytokine, myostatin, and the transcription factors SMAD2 and SMAD3 which mediate many of the effects of the TGF-β pathway. As shown in Figure 2.1C, starvation significantly reduced gene expression of *myostatin* (lean: 0.6 and obese: 0.8 fold) and *SMAD3* (lean: 0.4 and obese: 0.6 fold), but had no effect on

*SMAD2*. Similarly, dexamethasone significantly reduced *myostatin* (lean: 0.75 and obese: 0.83 fold) and *SMAD3* (lean: 0.75 and obese: 0.80 fold), but not *SMAD2*, gene expression. IGF-1 treatment did not significantly alter expression *myostatin*, *SMAD2*, nor *SMAD3*.

As shown in Figure 2.1D, there was a significant group effect (p=0.039) for *FoxO3* gene expression to be higher in the obese myotubes. Under basal conditions, *FoxO3* gene expression was 1.32 fold higher in obese myotubes. While the direction of change in *FoxO3* expression was similar between lean and obese in response to all experimental conditions, *FoxO3* gene expression was higher in the obese in response to IGF-1 (1.46 fold), dexamethasone (1.54 fold) and starvation (1.84 fold). However, the interaction between treatments and obesity failed to reach statistical significance (p=0.06). No other genes tested were differentially expressed between myotubes of the lean and severely obese.

**Protein degradation rates are similar between myotubes of the lean and severely obese**

In order to determine whether protein degradation rates differ between skeletal muscle of the lean and severely obese, we directly measured protein degradation rates in primary HSkMC myotubes in response to 24 h of IGF-1, dexamethasone, or starvation.

Compared to lean, the rate of protein degradation tended to be reduced in myotubes from obese (1.45 vs. 1.31%/h) under basal conditions, although this difference failed to reach statistical significance (p=0.15, Figure 2.2A). Likewise, basal protein synthesis was not different between myotubes of the lean and severely obese (Supporting information 2.2). Starvation significantly increased protein degradation rate (~40%), however, there was no significant interaction between starvation and obesity. IGF-1 treatment decreased protein degradation rates by approximately 10% in lean and 6% in severely obese, but this difference failed to reach statistical significance. Likewise, there was no significant effect of dexamethasone to increase protein degradation rate.

As shown in Figure 2.2B, myotubes from the lean and severely obese contained similar amounts of total protein under basal conditions. Following starvation, protein content of myotubes was significantly reduced to a similar extent (~20%) in myotubes from the lean and severely obese. Likewise, IGF-1 significantly increased protein content (~6%) similarly in myotubes from the lean and severely obese. Dexamethasone was insufficient to reduce protein content in either lean or severely obese.

**Differential flux through proteasome- and autophagy- mediated protein degradation**

Although total protein degradation rates were found to be similar, we next wanted to determine how obesity affects flux through the major protein degradation pathways, since these pathways preferentially target different proteins and/or organelles for

degradation (84). In order to accomplish this, we pooled myotubes from three lean and three obese individuals and measured protein degradation rates in response to proteasome inhibition (1.0μM PS-341, Bortezomib), lysosome acidification inhibition (0.1μM concanamycin A), or combined proteasome and lysosome inhibition. Inhibitor dosages were determined as the lowest dose effective to yield maximal inhibition during a dose-response experiment (Figure 2.3A).

In order to determine the rate of flux through the UPS and autophagic/lysosomal pathways, we subtracted inhibitor-sensitive protein degradation rate from the vehicle-treated total protein degradation rate (Figure 2.3B). The rates of flux through each pathway are depicted in Figure 2.3C. There was a significant group effect for myotubes of the severely obese to have decreased flux (basal -26%, starved -18%) through the autophagic/lysosomal pathway. Surprisingly, starvation reduced UPS flux by 19% in myotubes of the lean myotubes, but increased UPS flux by 4% in myotubes of the severely obese. This interaction was statistically significant, indicating a shift toward UPS-mediated protein degradation in myotubes of the severely obese during starvation. During starvation, flux through the autophagic/lysosomal pathway doubled in myotubes of the lean and severely obese. The magnitude of the differences in total, proteasomal, and lysosomal degradation rates are depicted in Figure 2.3D.

**Proteasome activity is increased in obese myotubes**

We next examined how severe obesity affects proteasome activity to determine whether this may explain the altered UPS flux during starvation. Therefore, we pooled

myotubes of three lean and of three obese individuals and subjected each pool to starvation for 24 h, then measured chymotrypsin-like activity of the purified proteasomes with the fluorogenic substrate Suc-LLVY-amc. The proteasome inhibitor PS-341 attenuated fluorescence in a dose-response manner (data not shown), indicating the specificity of this assay for proteasome activity.

As shown in Figure 2.4, there was a significant group effect for chymotrypsin-like activity of the proteasome to be higher in myotubes of the obese than lean. Starvation significantly increased proteasome activity in myotubes of the lean (30%) and severely obese (23%). However, there was no significant interaction between obesity and starvation on proteasome capacity.

**Myotubes from the lean and severely obese atrophy to a similar extent in response to starvation**

It is well-known that contractile elements of the sarcomere are degraded in a proteasome-dependent manner (18). Therefore, due to the altered UPS flux and proteasome capacity observed in severe obesity, we next sought to determine how obesity affects loss of myotube size during starvation. Myotubes were subjected to starvation for 24 h and myotube area quantified by immunofluorescence of myosin heavy chain (Figure 2.5A). Starvation was used as a model of atrophy due to the dramatic upregulation of protein degradation rate and loss of protein content (c.f. Figure 2.2). As shown in Figure 2.5, myotube area (2.5B), nuclei number (2.5C) and myotube area/nucleus (2.5D) were similar between lean and obese under basal conditions. As

expected, there was a significant main effect for starvation to decrease myotube area (~30%, $p<0.05$). Interestingly, there was also a significant main effect of starvation to reduce nuclei number (~15%), suggesting this treatment may also induce apoptosis, as has been described in mouse muscle myotubes (C2C12) (86). Despite the reduced number of nuclei following starvation, starvation significantly reduced myotube area/nucleus (~20%), demonstrating that loss of myotube size occurs to a greater extent than loss of nuclei number. However, there was no significant interaction between obesity and starvation on muscle atrophy. Following 24 h of starvation, myotube area and myotube area/nucleus were similar between myotubes of the lean and obese.

## Discussion

Contrary to our original hypothesis, we found no differences in absolute protein degradation rate between myotubes of the lean and severely obese, despite increased FoxO3 gene expression. Importantly, flux through the major protein degradation pathways, is altered in myotubes from the severely obese. To our knowledge, this is the first study to directly measure flux through the UPS and autophagic/lysosomal pathways of skeletal muscle from lean and severely obese humans. Given the distinct roles of the UPS and autophagic/lysosomal pathways (84), the specific proteins degraded during muscle atrophy may be substantially different between lean and severely obese skeletal muscle.

HSkMC myotubes are an excellent model with which to study protein metabolism in obesity. First, since the myoblasts are purified and passaged in culture for many weeks (5), cells from lean and obese individuals are subject to the same extracellular conditions. Therefore, the differences we observe are specific to skeletal muscle of lean and severely obese and not due to different cell types, circulating factors, or physical activity. Second, HSkMC myotubes, purified and passaged exactly as we have done here, retain many metabolic characteristics observed in vivo (43). For instance, HSkMC derived from severely obese individuals are insulin resistant (6) and have impaired fatty acid oxidation (10). Therefore, phenotypic differences in myotubes are likely to be present *in vivo*.

Compared to lean, both the absolute rate of flux through the autophagic/lysosomal pathway and its relative contribution to total protein degradation are decreased in myotubes from the extremely obese. The autophagic/lysosomal

pathway, but not the UPS, is responsible for the degradation of entire organelles, such as mitochondria. It has previously been observed that obesity is accompanied by impaired mitochondrial function (9). It is possible that decreased flux through the autophagic/lysosomal pathway may slow degradation of damaged or non-functional mitochondria within obese skeletal muscle. In support of this, Wu et al. (106) recently described impaired mitochondrial respiration and insulin resistance in mice with skeletal muscle deletion of Autoghapy-related gene 7 (Atg-7). Therefore, decreased autophagic/lysosomal pathway flux may represent not only impaired protein metabolism in obese skeletal muscle, but may also contribute to impaired carbohydrate and lipid metabolism. Future research should aim to discover the mechanistic causes and clinical significance of differential flux through the protein degradation pathways in obesity.

Additionally, we found that UPS flux is differentially regulated between lean and obese myotubes in response to starvation. Compared to lean, UPS flux was 13% lower in myotubes of the severely obese under basal conditions and 12% higher in response to starvation. The increased UPS flux in response to starvation indicates a shift toward UPS-mediated protein degradation in myotubes of the severely obese. It is well-known that the UPS mediates degradation of specific proteins, including contractile proteins (18). Despite elevated UPS flux, starved myotubes of the severely obese degrade proteins and lose myotube area at similar rates as those of lean individuals (c,f. Figure 2.2 and 2.5). However, it is possible that this shift may result in increased degradation of specific contractile proteins (18) and therefore contribute to lower specific force generation in muscles of the obese (44). Future research should examine whether

there is a preferential loss of specific contractile proteins in skeletal muscle of the severely obese during muscle atrophy.

UPS flux is determined by catabolic activity of the proteasome and protein polyubiquitination and deubiquitination (3, 104, 105). We determined that maximal proteasome activity is significantly greater in myotubes from obese individuals (c.f. Figure 2.4). Recently, several proteins have been identified that bind to, and modify, catabolic activity of the proteasome (21, 76). Therefore, it is possible that proteasome binding partners are differentially expressed in obese skeletal muscle. However, we noted that starvation increased proteasome activity to a similar extent in both lean and obese myotubes. Therefore, it is unlikely that proteasome activity alone can explain the elevated UPS flux seen in myotubes of the obese in response to starvation. Gene expression of two major E3 ubiquitin ligases essential for muscle protein degradation, *Atrogin-1* and *MuRF-1*, were similarly expressed in myotubes from the lean and severely obese under basal and starved conditions. However, it is possible that increased expression of other E3 ligases or increased ubiquitin ligase activity may explain the increased UPS flux in myotubes of the obese in response to starvation. Alternatively, decreased expression of deubiquitinating enzymes during starvation may increase UPS flux in myotubes of the obese. To date, few studies have examined the role of deubiquitinating enzymes during muscle atrophy, although several deubiquitinating enzymes are upregulated during muscle atrophy (3, 105).

Protein degradation responses are, at least in part, regulated at the level of gene transcription (25, 33). We noted a similar pattern of gene expression between lean and

obese myotubes under basal, IGF-1, dexamethasone, or starved conditions; all genes analyzed displayed a similar expression level between lean and obese myotubes with the exception of *FoxO3*, which was higher in the obese. *FoxO3* is known to activate muscle atrophy through upregulation of genes involved in both the UPS and the autophagic/lysosomal pathway (107). Interestingly, despite elevated *FoxO3* gene expression, we found similar expression patterns of the FoxO3-inducible genes *Atrogin-1*, *MuRF-1*, *LC3B*, and *Gabarapl-1* between lean and obese myotubes. This suggests obese skeletal muscle may be resistant to the atrophic effects of FoxO3. Transcriptional activity of FoxO3 is, in large part, dictated by Akt-mediated phosphorylation and cytosolic sequestration (93). Sishi et al. (91) determined FoxO phosphorylation is decreased in skeletal muscle of obese, pre-diabetic rats. Due to whole-body insulin resistance observed in our severely obese subjects (Table 2.1), it is reasonable to expect that FoxO3 phosphorylation may be reduced in these myotubes and therefore inhibit FoxO3-induced gene expression.

Taken together, our data indicate that skeletal muscle of the lean and severely obese atrophy at similar rates, but through different mechanisms. Specifically, skeletal muscle of the severely obese has decreased flux through the autophagic/lysosomal pathway under basal and starved conditions. Additionally, during starvation, skeletal muscle of the severely obese experiences a relative shift toward UPS-mediated protein degradation. Despite differential flux through the UPS and autophagic/lysosomal pathways, total loss of myocellular size and total protein degradation rates are similar between skeletal muscle of the lean and severely obese in response to starvation. Myotubes of the severely obese overexpress *FoxO3*, a transcription factor largely

responsible for increasing transcription of genes involved in both the UPS and the autophagic/lysosomal pathway, however, gene expression patterns of FoxO3-inducible genes are similar between myotubes of the lean and severely obese.

**Acknowledgements**

Funding for this project was provided by Start-up funds from East Carolina University to JJB, Start-up funds from East Carolina University to CAW, NIH RO1-DK56112 to JAH, and a pre-doctoral award from the American College of Sports Medicine Foundation to LMB. The authors would like to thank Jonathan Powell and Dr. Jill Maples for their excellent technical contributions to this work

## Tables and Figures

| | n | Age | BMI | Fasting glucose (mg/dl) | Fasting insulin (μIU/ml) | HOMA-IR |
|---|---|---|---|---|---|---|
| Lean | 10 | 24.2 ± 1.5 | 22.9 ± 0.8 | 85.2 ± 2.6 | 9.3 ± 1.1 | 1.65 ± 0.2 |
| Obese | 8 | 34.1 ± 3.3* | 46.9 ± 2.1* | 93.7 ± 2.9 | 18.2 ± 2.2* | 4.27 ± 0.6* |

**Table 2.1. Subject characteristics.** Data are presented as mean ± SEM. BMI = body mass index ($kg/m^2$). * Significantly different from lean ($p<0.05$).

| | Gene | | Sequence (5' → 3') |
|---|---|---|---|
| TGF-β pathway | Myostatin | Fwd | AAGACCAAAATCCCTTCTGGA |
| | | Rev | CTGTAACCTTCCCAGGACCA |
| | SMAD2 | Fwd | TGTTCTTACCAAAGGCAGCA |
| | | Rev | CATCGGAAGAGGAAGGAACA |
| | SMAD3 | Fwd | GTAGCTCGTGGTGGCTGTG |
| | | Rev | AACACCAAGTGCATCACCAT |
| Ubiquitin-proteasome system | FoxO3 | Fwd | CTCTTGCCAGTTCCCTCATT |
| | | Rev | CTTCAAGGATAAGGGCGACA |
| | Atrogin-1 | Fwd | TCAGGGATGTGAGCTGTGAC |
| | | Rev | GGGGGAAGCTTTCAACAGAC |
| | MuRF-1 | Fwd | CTTCGTGCTCCTTGCACAT |
| | | Rev | ATCGTCACGGAGTGTACGG |
| Autophagy | LC3B | Fwd | TATCACCGGGATTTTGGTTG |
| | | Rev | GAGAAGACCTTCAAGCAGCG |
| | ATG4B | Fwd | AGTATCCAAACGGGCTCTGA |
| | | Rev | ACTGGGAAGATGGACGCAG |
| | Gabarapl-1 | Fwd | TGGCTTTTGGAGCCTTCCT |
| | | Rev | CCATCCCTTTGAGTATCGGA |
| Control gene | RPLPO | Fwd | AGGCGTCCTCGTGGAAGTGACA |
| | | Rev | TGCTGCATCTGCTTGGAGCCC |

**Table 2.2. Primers used for RT-PCR.**

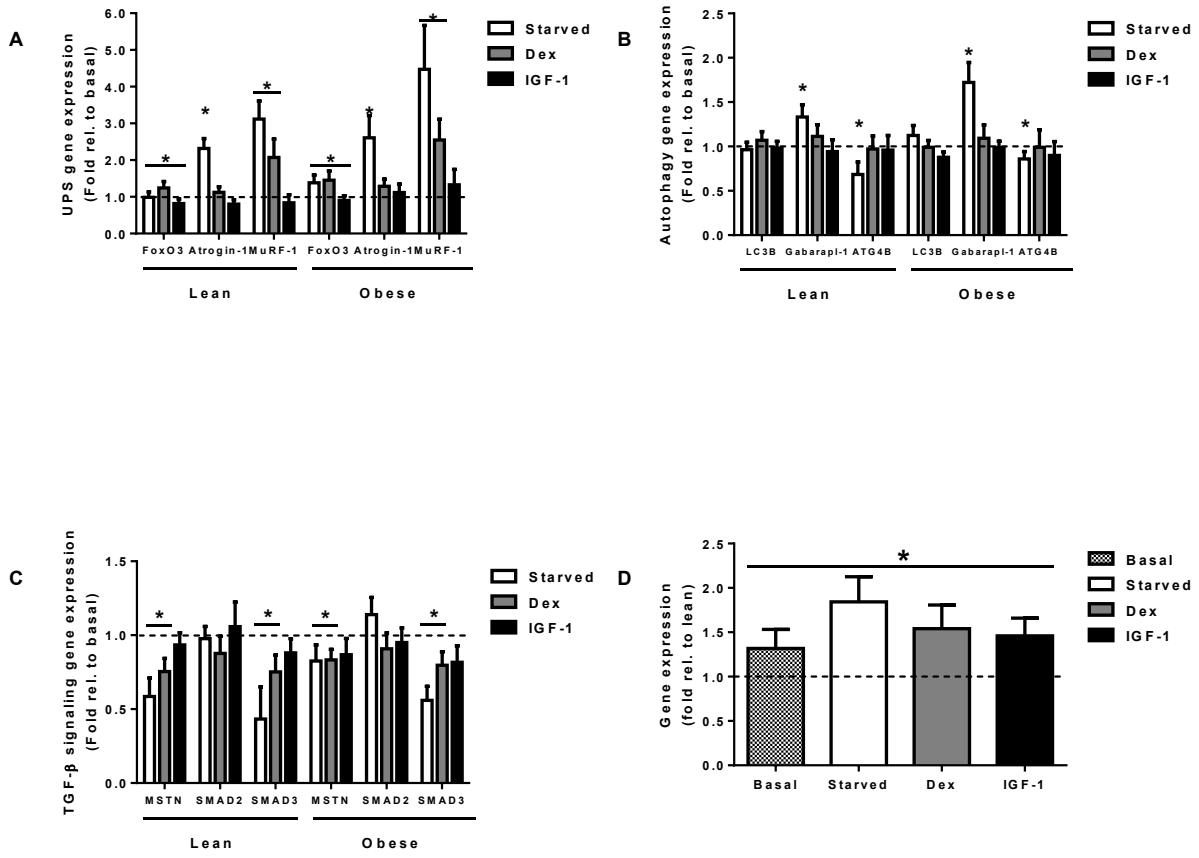


**Figure 2.1. IGF-1, dexamethasone, and starvation alter atrophy-related gene expression in myotubes of lean and severely obese.** Myotubes were treated for 24 h, RNA was collected, and RT-PCR was performed. A: Genes involved in the ubiquitin-proteasome system (UPS). B: Genes involved in the autophagic/lysosomal pathway. C: Genes involved in Transforming Growth Factor-β (TGF-β) signaling. D: FoxO3 gene expression of obese myotubes expressed as fold relative to lean. Fold changes were calculated using the relative standard curve method. Data are presented as mean ± SEM. * Significant main effect of treatment ($p<0.05$).

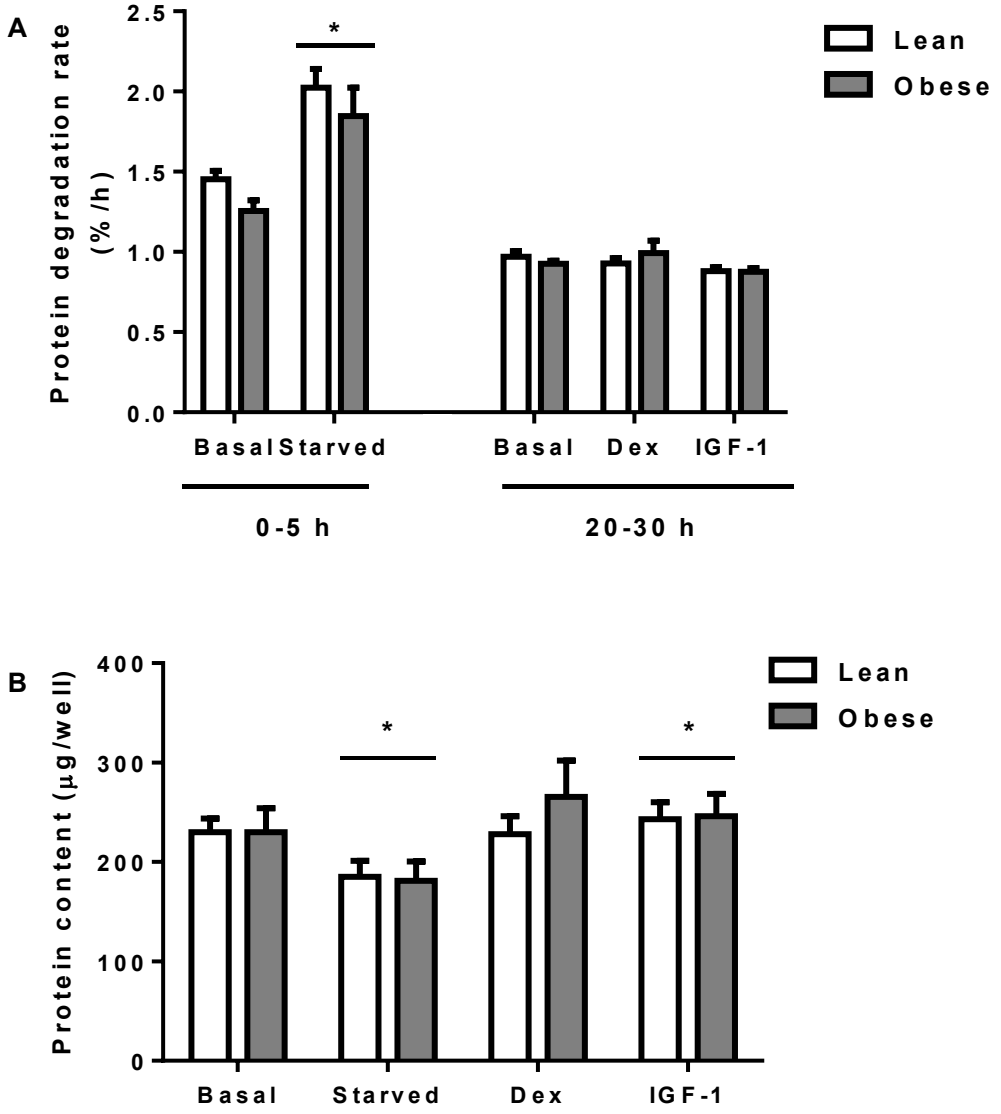


**Figure 2.2. Protein degradation rates of lean and obese myotubes respond similarly to atrophic and hypertrophic stimuli.** A: Protein degradation rate: myotubes were labeled with $^{3}$H-tyrosine for 24hr then subjected to starvation, dexamethasone, or IGF-1. Protein degradation rate was calculated by the amount of $^{3}$H in media samples collected over the course of 5hr (starved) or 20-30hr (IGF-1, dexamethasone). Each data point is the mean of four replicates. B: Protein content: myotubes were subjected to treatments for 24 h and protein content determined by BCA assay. Data are presented as mean ± SEM. * Significant main effect of treatment ($p<0.05$).

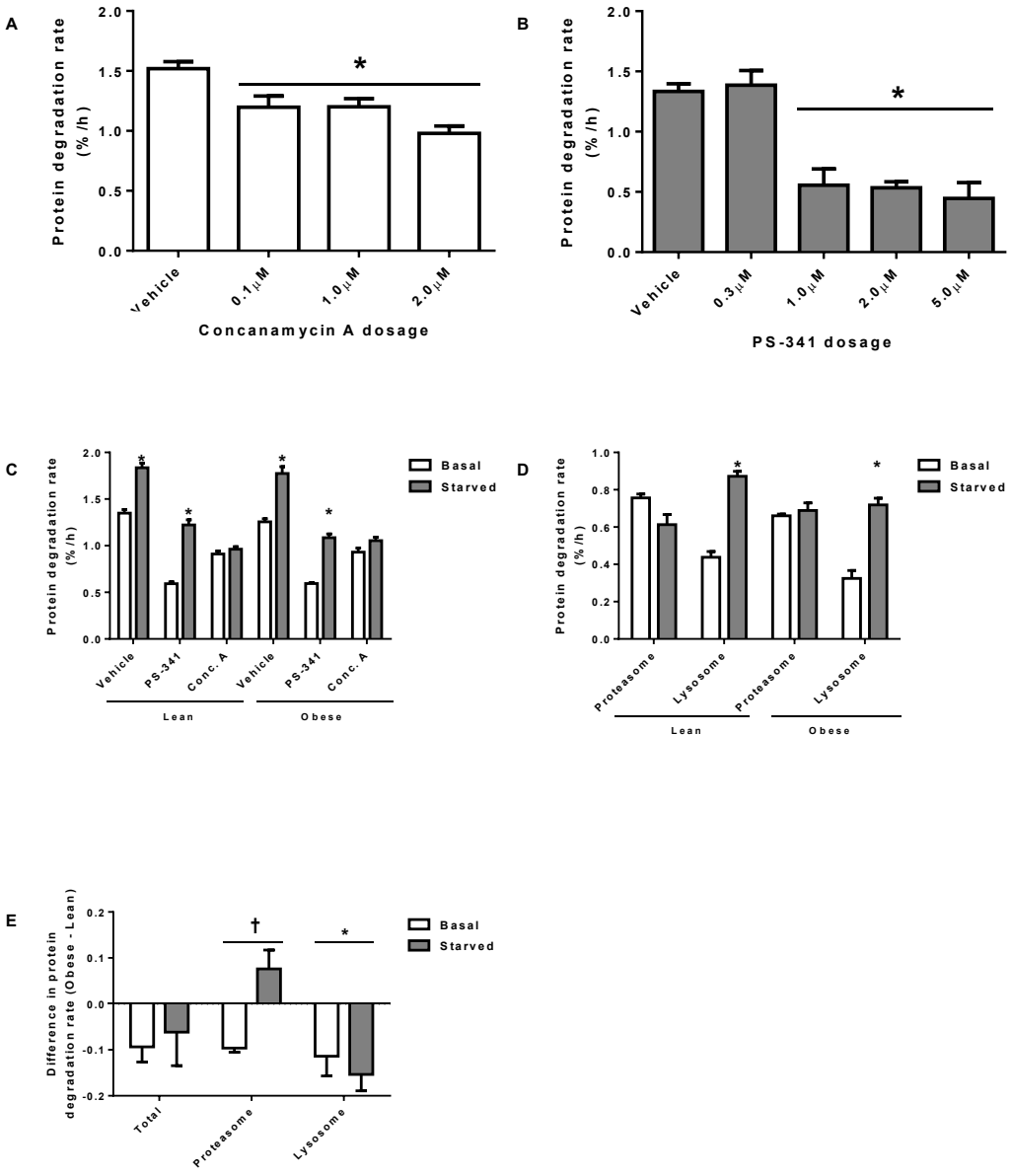


**Figure 2.3. Flux through the ubiquitin-proteasome system and autophagic/lysosomal pathway is altered in myotubes from the severely obese.** Pooled myotubes (three individuals per group) were treated with the proteasome inhibitor PS-341 and/or the lysosome inhibitor Concanamycin A, incubated in serum and amino acid free media, and protein degradation rates determine by $^{3}$H-tyrosine release. A-B: Dose-response curves for inhibitors used. C: Protein degradation rates in response to inhibitors. D: Inhibitor-sensitive proteolysis was determined by subtracting the degradation rate in the presence of inhibitors from vehicle-treated controls. E: Differences in protein degradation rates were determined by subtracting values of lean from obese (Δ Degradation rate = degradation rate$_{obese}$ – degradation rate$_{lean}$). Data are presented as mean ± SEM. * Significant main effect of treatment ($p<0.05$). † Significant main effect between groups ($p<0.05$). § Significant interaction effect ($p<0.05$).

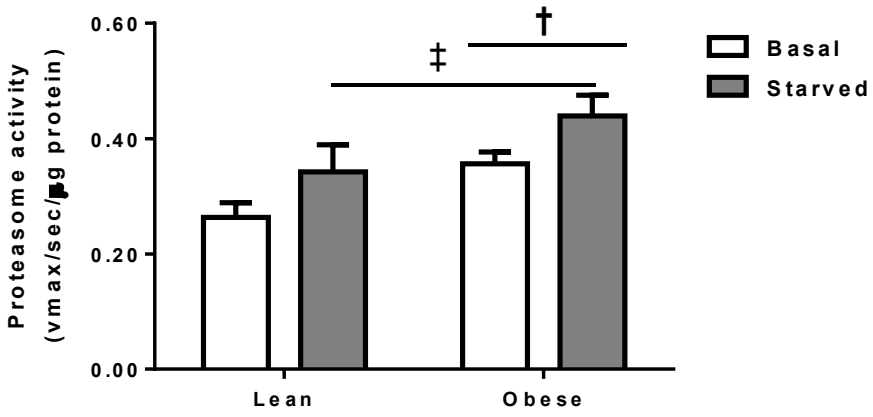


**Figure 2.4. Proteasome activity is increased in myotubes from the severely obese.** Chymotrypsin-like activity was assessed by the fluorogenic substrate Suc-LLVY-amc. ‡ Significant main effect (basal vs starved, $p<0.05$). † Significant main effect (lean vs obese, $p<0.05$).

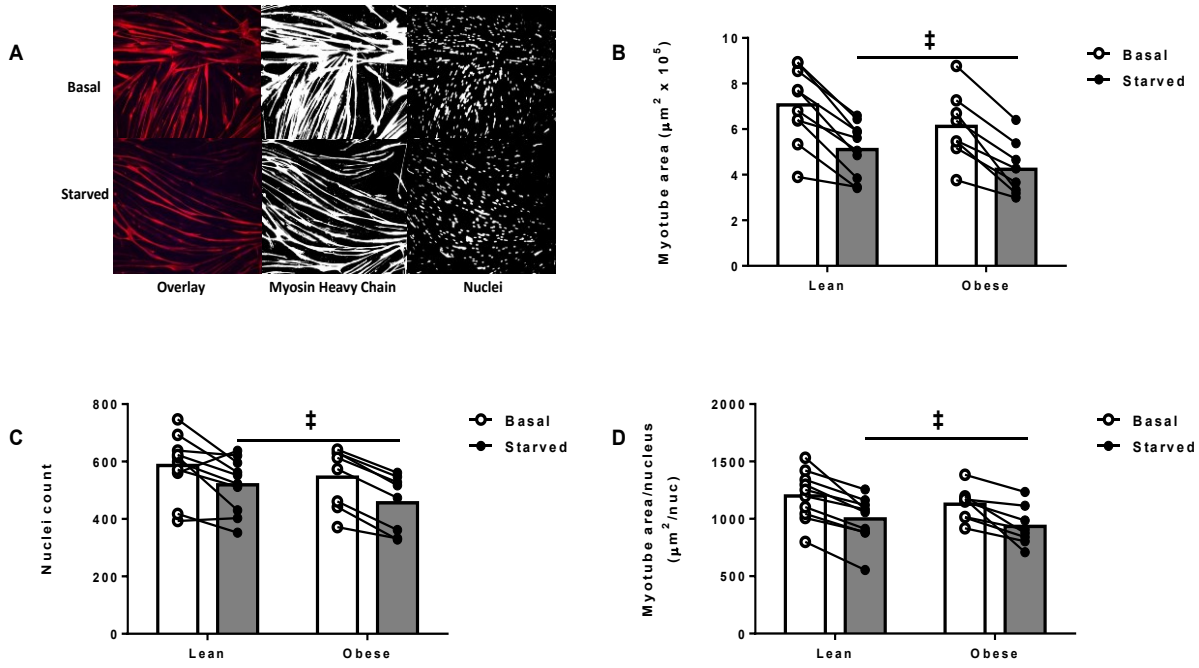


**Figure 2.5. Myotubes from lean and severely obese atrophy at similar rates.** A: Representative two-colored fluorescent images stained for both myosin heavy chain and nuclei (*Overlay*). Images were split from RGB format to individual components and converted to threshold images representing *Myosin Heavy Chain* and *Nuclei*, B: Myotube area ($\mu m^2$). C: Number of nuclei. D: Myotube area per nucleus ($\mu m^2$/nucleus). Individual data points are presented. ‡ Significantly different vs basal ($p<0.05$).

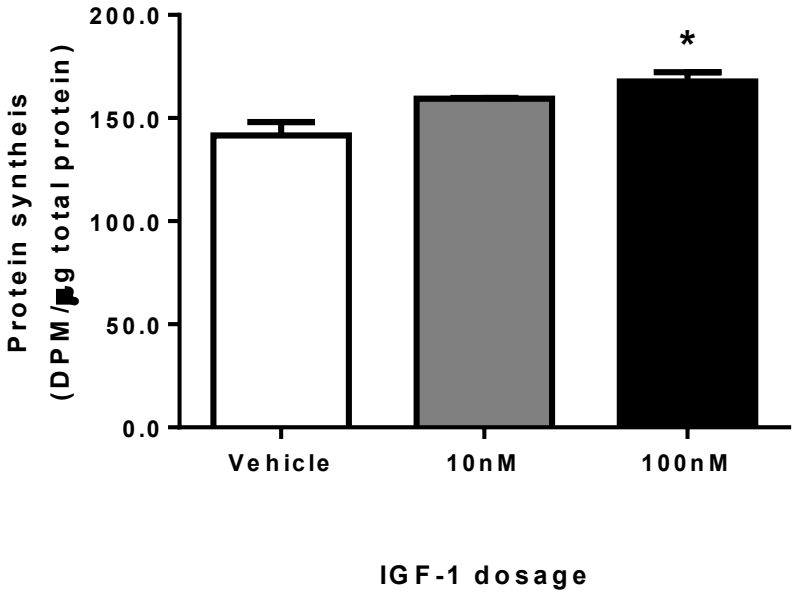


**Supporting information 2.1: 100nM IGF-1 increases rate of protein synthesis in HSkMC myotubes.** Myotubes were treated with vehicle (HCl), 10nM IGF-1, or 100nM IGF-1 for 24 h then radiolabeled with 5µCi/ml $^{3}$H-tyrosine for 2 h, cellular proteins precipitated by 10% TCA, washed in 95% ethanol, and solubilized in 0.2N NaOH. TCA precipitable radioactivity was determined by scintillation counting and normalized to total protein (assessed by bicinchoninic acid assay). Data are presented as mean ± SEM. n=3 per condition. * Significantly different vs vehicle, $p<0.05$

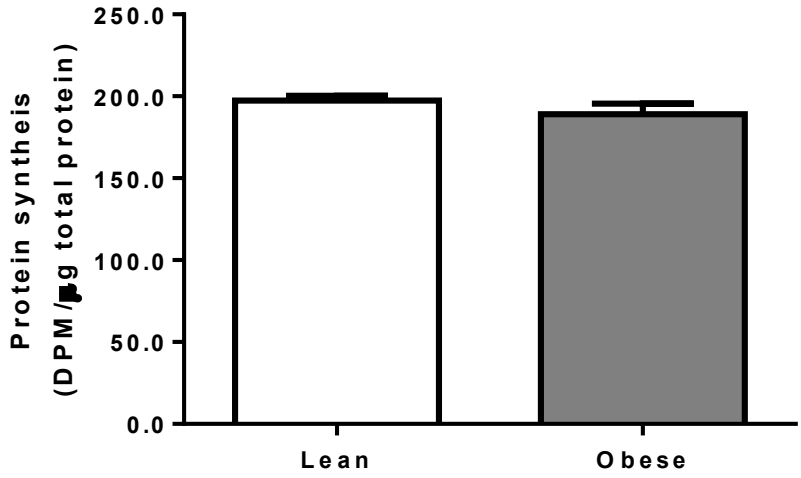


**Supporting information 2.2: Basal protein synthesis rate is similar between myotubes of lean and severely obese women.** Pooled myotubes (four per group) were radiolabeled with 5µCi/ml $^{3}$H-tyrosine for 2 h, cellular proteins precipitated by 10% TCA, washed in 95% ethanol, and solubilized in 0.2N NaOH. TCA precipitable radioactivity was determined by scintillation counting and normalized to total protein (assessed by bicinchoninic acid assay). Six replicates were performed per group.

# Chapter 3: SMAD3 regulates FoxO-induced MuRF-1 gene transcription via dual mechanisms


## Abstract

During muscle atrophy, Muscle-specific RING Finger-1 (MuRF-1) targets muscle contractile proteins for rapid degradation. The transcription factors SMAD3 and FoxO independently increase transcription of protein degradation genes and cause muscle atrophy. However, it is not known whether these transcription factors coordinately regulate transcription of ubiquitin ligases. It is possible that these transcription factors synergistically increase transcription of ubiquitin ligases during muscle atrophy. The purpose of the current project was to determine the additive effects of these transcription factors on ubiquitin ligase gene transcription. **Methods:** C2C12 myotubes were infected with adenoviruses encoding for SMAD3 and/or FoxO3 and gene expression of *Atrogin-1* and *MuRF-1* measured by RT-PCR. Human embryonic kidney (HEK293a) cells were co-transfected with plasmid DNA encoding MuRF-1 luciferase reporters (wt or SBE-mutant), FoxO1, FoxO3, and/or SMAD3. **Results:** Overexpression of FoxO3 increased gene expression of *Atrogin-1* and *MuRF-1* and this effect was synergistically increased by co-expression of SMAD3. Co-expression of FoxO3 and SMAD3 synergistically increased FoxO3 and SMAD3 DNA interactions and *MuRF-1* promoter activity. Mutagenesis of the SMAD binding elements eliminated SMAD3-DNA interactions and significantly attenuated FoxO3-DNA interactions and FoxO-induced *MuRF-1* promoter activity, suggesting SMAD3 is essential for optimal FoxO-induced transcription of *MuRF-1*. SMAD3 overexpression increased FoxO3 protein content in a dose-dependent manner, but had no effect on FoxO1 or FoxO3

mRNA. Co-expression of FoxO3 and SMAD3 synergistically increased FoxO-dependent gene transcription as indicated by FRE-driven luciferase activity. **Conclusions:** SMAD3 synergistically increases FoxO-induced transcription of the ubiquitin ligases *Atrogin-1* and *MuRF-1*. SMAD3 appears to be essential for optimal FoxO-induced MuRF-1 gene transcription by increasing FoxO binding to the proximal promoter region. Additionally, SMAD3 overexpression increases protein content and transcriptional activity of FoxO, possibly by inhibiting degradation of FoxO protein. We conclude that SMAD3 regulates gene transcription of ubiquitin ligases through a dual effect on FoxO: 1) increasing FoxO protein content and transcriptional activity and 2) increasing FoxO binding at conserved FRE-SBE motifs within the proximal promoter region.

## Introduction

Skeletal muscle mass is dictated by the balance between protein synthesis and degradation rates (34). Severe loss of muscle mass, or muscle atrophy, is characterized by an increased protein degradation rate. This is especially true for ubiquitin proteasome system (UPS)-mediated protein degradation (46). Numerous forms of muscle atrophy activate a common transcriptional program to induce expression of genes involved in protein degradation, including the ubiquitin ligases *Atrogin-1* and Muscle-specific RING Finger-1 (*MuRF-1*) (54, 78, 82). Atrogin-1 promotes degradation of eukaryotic translation initiation factor 3F (eIF3-F) (20) as well as desmin and vemintin (58). During muscle atrophy, MuRF-1 targets contractile proteins of the thick filament for degradation (18), thereby contributing to both decreased skeletal muscle mass and decreased muscle force development. Furthermore, these ubiquitin ligases are essential for muscle atrophy (8) and are known to be, at least in part, transcriptionally regulated (54). Unfortunately, the cellular mechanisms regulating transcription of *Atrogin-1* and *MuRF-1* are incompletely understood.

*Atrogin-1* and *MuRF-1* gene expression is clearly regulated, at least in part, by the transcription factor Forkhead box type O (FoxO) (81, 87, 100). FoxO1 and 3 are sufficient to induce protein degradation (83, 107), *Atrogin-1* (83) and *MuRF-1* gene expression (87, 100), and ultimately, muscle atrophy. FoxO recognizes the FoxO Response Element (FRE, (A/G)TAAA(T/C)A) within the promoter region to induce transcription of *Atrogin-1* and *MuRF-1* (83, 100). Interestingly, the synthetic glucocorticoid dexamethasone synergistically increases FoxO-induced MuRF-1

promoter activity (100), suggesting that FoxO may require DNA binding partners to fully activate the MuRF-1 promoter region.

One potential FoxO DNA binding partner is SMAD3, a transcription factor activated by the Transforming Growth Factor-β (TGF-β) pathway. A recent meta-analysis of human and rodent microarray studies implicated the TGF-β pathway as the core pathway and SMAD3 as a major signaling node for general muscle atrophy (13). Gene expression of *Atrogin-1* and *MuRF-1* is increased following administration of the TGF-β family member myostatin in vitro (56, 57). Overexpression of SMAD3 induces muscle atrophy and *Atrogin-1* gene expression, but is insufficient to induce *MuRF-1* gene transcription *in vitro* (35) or *in vivo* (85). Therefore the direct role of SMAD3 transcriptional regulation of ubiquitin ligases is somewhat controversial. SMAD3 regulates FoxO activity by inhibiting Akt-mediated phosphorylation (and cytosolic sequestration) of FoxO (4, 67, 99). FoxO and SMAD transcription factors have previously been shown to physically associate and synergistically regulate the cyclin-dependent kinase inhibitor p21Cip1 gene expression (88). Furthermore, of 115 genes regulated by TGF-β in keratinocytes, 11 require FoxO as a DNA binding partner (33). Therefore, it is possible that SMAD3 may modulate FoxO-induced transcription of muscle-specific ubiquitin ligases.

Both SMAD3 and FoxO transcription factors are known to be major regulators of the transcriptional program that induces muscle atrophy (37). The effects of these transcription factors on atrophy have largely been studied independently; the effects of the interaction between these transcription factors have not been well characterized. The purpose of the present study was to determine how FoxO- and SMAD3- DNA

interactions coordinately regulate gene expression of muscle-specific ubiquitin ligases. Since it has previously been reported that SMAD3 and FoxO coordinately regulate several genes, we hypothesized that SMAD3 functions to augment FoxO-dependent gene transcription of ubiquitin ligases.

**Methods:**

**Cell culture:**

Primary human skeletal muscle myoblasts (HSkMC) were generated as previously described (5) by isolating satellite cells from muscle biopsies of the vastus lateralis from four female subjects. Myoblasts were pooled and cultured together in Dulbecco's modified Eagle's medium (DMEM) supplemented with 10 % fetal bovine serum, rhEGF, dexamethasone, gentamycin, BSA, and fetuin (SkGM Singlequots, Lonza). Upon reaching confluence, growth media was switched to low serum media (2 % horse serum) supplemented with 3 % BSA and 0.1 % fetuin to induce differentiation into myotubes. Experiments were performed on day 6 of differentiation using two independent pools.

Human Embryonic Kidney (HEK, 293a) cells were cultured in DMEM supplemented with 10 % fetal bovine serum and 1 % penicillin/streptomycin. For all experiments, cells were seeded into six well plates at a density of $2.5 \times 10^5$ cells per well and allowed to adhere to the plate overnight.

Mouse skeletal muscle myoblasts (C2C12) were cultured in DMEM supplemented with 10 % fetal bovine serum and 1 % penicillin/streptomycin and maintained at sub-confluent density prior to differentiation. For all experiments, myoblasts were seeded into six well plates at a density of $2.5 \times 10^5$ cells per well and allowed to adhere to the plate overnight. Growth media was switched to low serum media (2 % horse serum) to induce differentiation into myotubes. Experiments were

performed on day 5 of differentiation. All cell cultures were maintained at 37°C and 5 % $CO_2$ and media was changed every 48 h.

**Protein Degradation Rate:**

Protein degradation rates were determined by release of a radiolabeled amino acid as previously described (11). Terminally differentiated myotubes were radiolabeled with L-[3,5-$^3$H] tyrosine (5 µCi/ml, PerkinElmer Life Sciences) for 24 h. Cells were thoroughly washed and radioactivity chased for 2 h using differentiation media supplemented with 2 mM L-tyrosine to allow degradation of short-lived proteins and to limit re-incorporation of the radiolabel. Myotubes were then subjected to atrophic stimuli. For HSkMC experiments, myotubes were incubated in media lacking serum (DMEM only), lacking amino acids (HBSS+2 %HS), or lacking both serum and amino acids (HBSS only). Four serial media samples were collected over the course of 5 h. At the end of the experiments, culture media was removed completely and myotubes were solubilized in 0.2N NaOH. Radioactivity of cells and TCA precipitated media samples was measured using scintillation counting. Total radioactivity was calculated as the sum of the residual radioactivity in the myotubes plus radioactivity of all time points. Protein degradation rate was directly calculated as a percentage of total [$^3$H] tyrosine incorporation from the regression line of serial samples for each individual.

**RT-PCR:**

HSkMC myotubes were subjected to atrophic conditions as described above for 24 h. C2C12 myotubes (d4 differentiation) were infected with adenovirus expressing

human wtSMAD3 (ad-wtSMAD3, Vector biosystems) for 24 h, then co-infected with adenovirus encoding human wtFoxO3 (ad-wtFoxO3, gift of Dr. Alfred Goldberg, University of Harvard Medical School) for an additional 24 h. Myotubes were washed twice with PBS and RNA collected using TRIzol (Ambion). RNA was stored at -80°C until processing. RNA integrity was determined by agarose gel electrophoresis. RNA concentration and purity (Ab260/280) was assessed spectrophometrically using a NanoDrop UV-Vis spectrophometer (ThermoScientific, ND-1000). RNA was reversed transcribed to cDNA (Quanta Biosciences) at a final concentration of 0.10 μg/μl. For both HSkMC and C2C12 experiments, Large Ribosomal Protein (RPLPO) was used as an endogenous control gene and fold expression was calculated using the ΔΔCt method. Custom RT-PCR primers (Table 3.1) were generated using NCBI BLAST algorithms (http://blast.ncbi.nlm.nih.gov/Blast.cgi) and specificity confirmed by agarose gel electrophoresis following conventional PCR. All RT-PCR experiments were run with a standard curve of eight orders of magnitude and amplification efficiency was determined to be near 100%.

**Luciferase Reporter Assay**

**Plasmid vectors**

Plasmids encoding wild type human FoxO1 (97), FoxO3 (79), SMAD3 (52), and dominant-negative SMAD3 (dnSMAD3) (16), were purchased from addgene (addgene plasmids13507, 10710, 11742, and 12638 respectively). The FoxO Response Element reporter (FRE-luc) was a kind gift of Dr. Marco Sandri (Dulbecco Telethon Institute) (83). The 5kb pGL3 wtMuRF-1 reporter (mouse) was a kind gift of Dr. Monte S. Willis

(University of North Carolina School of Medicine). This reporter has previously been used to examine MuRF-1 promoter activity both *in vivo* (85) and *in vitro* (100). The promoter region of this plasmid was confirmed by DNA sequencing and aligned against the human *MuRF-1* promoter region using NCBI algorithms (http://blast.ncbi.nlm.nih.gov) to identify conserved sequences. Site-directed mutagenesis (Stratagene) of two putative SMAD-binding elements (SBE, AGAC) within the proximal promoter region (5 and 11 bp upstream of the transcriptional start site) was performed to generate a 5kb mutant MuRF-1 reporter (SBE-mut). These AGAC sequences were mutated to AGgg and AtcC as described by Seoane et al (88). Both the 5kb wild type and 5kb SBE-mut reporters were truncated to approximately 2kb (digested with NheI and NdeI) and 0.25kb (digested with NheI and PstI) followed by blunt-end ligation (New England Biolabs). The promoter regions of these reporters were sequenced and aligned against the wild type reporter to confirm effective mutagenesis.

**Luciferase assay**

HEK cells were transfected with 2.0μg (including 0.25μg reporter DNA) of total plasmid DNA per well using FuGene 6 per manufacturer's recommendations (Promega). An eGFP plasmid was used as a transfection control and to balance total DNA transfection between conditions. Experiments were performed 48 h post-transfection. Cells were washed twice with PBS and collected in 1x passive lysis buffer per manufacturer's recommendation (Promega). Samples were spun at 20,000 x g for

5 min and 20 µl of the supernatant pipetted into a white 96-well plate with 100 µl of substrate. Luminescence was measured using a microplate reader (Spectramax M4). Luciferase values were normalized to total protein content as measured by bicinchoninic acid (BCA) assay (ThermoScientific) and expressed as fold relative to eGFP transfected cells.

**Chromatin Immunoprecipitation**

HEK cells were plated in 10cm dishes (n=6 per group) at a density of $2.0x10^6$ cells per dish allowed to adhere overnight, then transfected with plasmid DNA encoding either wt or SBE-mut 0.25kb MuRF-1 reporter and 1) eGFP, 2) wtFoxO3, 3) SMAD3, or 4) wtFoxO3 + wtSMAD3. Forty-eight hours after transfection, proteins were cross-linked with chromatin using 1% formaldehyde and DNA was collected. DNA was sheared by sonication to approximately 1kb fragments and antibodies against FoxO3 (Cell Signaling #2497), SMAD3 (Cell Signaling #9523), or IgG (negative control) were used to immunoprecipitate DNA. After cross-linking was reversed, RT-PCR was performed for the proximal region of the 0.25kb MuRF-1 reporter using primers flanking the FRE-SBE motif. Using primers specific for the reporter accomplished our three-fold goal: 1) confirming mutagenesis eliminated SMAD3 binding within the MuRF-1 promoter region, 2) bypassing epigenetic modifications, such as CpG methylation that may prevent MuRF-1 expression in HEK cells, and 3) eliminating effects of secondary and tertiary DNA structure on DNA binding.

**Western blotting:**

C2C12 myotubes were infected with adenoviruses encoding GFP or SMAD3 (Vector Biosystems) for 24 h. Cells were washed twice with PBS and protein collected using freshly made Radio-Immunoprecipitation Assay (RIPA) buffer containing 1% NP-40, 0.5% sodium deoxycholate, 0.1% SDS, and protease inhibitor cocktail (Roche Complete Mini). Samples were vortexed continuously for 1min, rotated end-over-end for 30 min, then centrifuged at 12,000 x g for 10min and the pellet discarded. Proteins were separated by SDS-PAGE, transferred to a polyvinylidene difluoride membrane and incubated with primary antibodies against FoxO3 (Cell Signaling #2497, 1:1000) or SMAD3 (Cell Signaling #9523, 1:5000) overnight. Secondary antibodies were conjugated to horseradish peroxidase and detected using an ECL substrate (Millipore). Band imaging and analysis was performed using a Bio-Rad Chemi Doc XRS and Image Lab software.

**Statistics:**

Data are presented as mean ± SEM. Statistical significance ($p<0.05$) was assessed using analysis of variance (ANOVA) followed by Tukey's honestly significant difference post-hoc test when appropriate. All analyses were performed using SPSS version 19.0.

## Results:

### Starvation increases protein degradation rate and ubiquitin ligase gene expression in vitro

In order to determine the response of ubiquitin ligases to muscle atrophy, we measured protein degradation rate and gene expression of *Atrogin-1* and *MuRF-1* in primary HSkMC myotubes in response to three atrophic stimuli. As expected, serum starvation, amino acid starvation, or combined serum and amino acid starvation increased protein degradation rates relative to basal in a step-wise manner (Figure 3.1A). Likewise, atrophy stimulation increased gene expression of both *Atrogin-1* (Figure 3.1B) and *MuRF-1* (Figure 3.1C) in a step-wise manner. Gene expression of both *Atrogin-1* and *MuRF-1* was increased following 5 h of atrophy stimulation. Although the magnitude of the effect was decreased, gene expression of *Atrogin-1* and *MuRF-1* remained elevated following 30 h of atrophy stimulation. Thus increased gene expression of *Atrogin-1* and *MuRF-1* is a robust and early response to atrophy stimulation in human skeletal muscle.

### SMAD3 and FoxO3 synergistically regulate transcription of *Atrogin-1* and *MuRF-1*

In order to determine the additive effects of SMAD3 and FoxO3 co-expression on transcription of ubiquitin ligases, we measured *Atrogin-1* and *MuRF-1* gene expression in C2C12 myotubes infected with ad-wtSMAD3 and/or ad-wtFoxO3. As shown in Figure 3.2A, wtFoxO3, but not wtSMAD3, significantly increased gene expression of *Atrogin-1*. Co-expression of wtFoxO3 and wtSMAD3 increased *Atrogin-1* gene expression to a

greater extent than wtFoxO3 alone. Similarly, overexpression of wtFoxO3, but not SMAD3, increased *MuRF-1* gene expression and co-expression of wtFoxO3 and wtSMAD3 increased *MuRF-1* gene expression to a greater extent than wtFoxO3 alone (Figue 3.2B). Together, this data indicates that FoxO3 and SMAD3 synergistically increase gene expression of *Atrogin-1* and *MuRF-1*.

Examining the promoter regions of *Atrogin-1* and *MuRF-1* in the mouse genome revealed that putative SBEs occur within close proximity (9-31 bp) of consensus FREs within the proximal promoter regions of both genes (FRE-SBE motif). The spacing between these binding sites is similar to that found for other genes coordinately regulated by SMAD and FoxO transcription factors (2, 33). In the mouse *Atrogin-1* promoter region, we found three such FRE-SBE motifs within 1.5 kb upstream of the transcriptional start site including one located 2 bp upstream of the transcriptional start site. In the human *Atrogin-1* promoter region, we found one FRE-SBE motif located 22 bp upstream of the transcriptional start site. Using open-access software, we were unable to determine any highly conserved sequences between mouse and human genomes in the *Atrogin-1* promoter region. In the mouse *MuRF-1* promoter region, we identified two FRE-SBE motifs within 1.5 kb of the transcriptional start site. Aligning the promoter regions of the *MuRF-1* gene (TRIM62) revealed the proximal 0.25kb of the *MuRF-1* gene is highly conserved (83% homology) between mouse and human genomes. Furthermore, one FRE-SBE motif, located 2 bp from the transcriptional start site is entirely conserved between species (Figure 3.3A). Therefore, we focused on the *MuRF-1* gene in order to determine the mechanistic action mediating the synergistic effects of SMAD3 and FoxO3.

In order to determine whether the synergistic effect of SMAD3 and FoxO is mediated by increased *MuRF-1* promoter activity, we co-transfected HEK cells with a 5kb wtMuRF-1 reporter, wtFoxO1, wtFoxO3, and/or wtSMAD3 plasmid DNA (Figure 3.3B). Overexpression of wtFoxO3, but not wtFoxO1, significantly increased MuRF-1 promoter activity. As previously reported (35, 85), overexpression of wtSMAD3 had no effect on *MuRF-1* promoter activity. Co-expression of wtFoxO1 + wtSMAD3 or wtFoxO3 + wtSMAD3 increased *MuRF-1* promoter activity to a greater extent than wtFoxO1 or wtFoxO3 alone, indicating a synergistic effect of these transcription factors on MuRF-1 promoter activity.

**The proximal 0.25kb MuRF-1 promoter region is a major regulator of transcriptional activity**

In order to determine the contribution of the proximal 0.25kb promoter region and the FRE-SBE motif to *MuRF-1* promoter activity, we created a series of reporters through site-directed mutagenesis (SBE-mut, AGACCAAGAC→AGggCAAtcC) and restriction digestion (5kb, 2kb, and 0.25kb) of the 5kb MuRF-1 luciferase reporter (Figure 3.3C). These reporters were co-transfected into HEK cells and basal promoter activity measured (Figure 3.3D). The wt2kb reporter retained 100% of basal transcriptional activity, while the wt0.25kb reporter retained 37% of basal transcriptional activity indicating the highly conserved proximal 0.25kb promoter region is a major determinant of basal *MuRF-1* promoter activity. Interestingly, the SBE-mut reporters

(5kb, 2kb, and 0.25kb) all retained basal promoter activity similar to their respective wild type reporters.

**SMAD3 augments FoxO3-induced *MuRF-1* transcription in a DNA-binding dependent manner**

In order to determine the mechanism of the synergistic effect of FoxO3 and SMAD3 on *MuRF-1* promoter activity, we co-transfected HEK cells with the 0.25kb MuRF-1 reporter (wt or SBE-mut), wtFoxO3, and/or wtSMAD3 (Figure 3.4). As expected, overexpression of wtFoxO3 significantly increased *MuRF-1* promoter activity in the wild type reporter. However, FoxO3-induced *MuRF-1* promoter activity was significantly attenuated in the SBE-mut reporter. Similar results were found when overexpressing FoxO1 (data not shown). Unlike the 5kb reporter, overexpression of wtSMAD3 alone significantly increased promoter activity in both the wild type and SBE-mut 0.25kb reporters. Furthermore, co-expression of wtFoxO3 and wtSMAD3 did not significantly increase MuRF-1 gene transcription compared to FoxO3 alone in either the wt or SBE-mut reporters which may be due to elimination of the upstream FRE-SBE motif from the MuRF-1 promoter region. In order to confirm these results, we overexpressed dnSMAD3 (lacking the DNA binding region) alone or in conjunction with wtFoxO3. Unlike wtSMAD3, overexpression of dnSMAD3 did not significantly increase *MuRF-1* promoter activity, but did significantly attenuate FoxO3-induced *MuRF-1* promoter activity. Based on these results, we hypothesized that SMAD3 binding to DNA augments, and is required for optimal, FoxO binding to the MuRF-1 promoter regions at FRE-SBE motifs.

In order to determine how SMAD3 affects FoxO3-DNA interactions, we performed chromatin immunoprecipitation (ChIP) of the 0.25kb MuRF-1 reporter. As expected, SMAD3 overexpression increased SMAD3 binding within the wt (Figure 3.5A), but not the SBE-mut (Figure 3.5B) reporter. Interestingly, co-expression of wtFoxO3 and wtSMAD3 dramatically increased SMAD3 binding to DNA in both the wt and SBE-mut reporters (Figure3. 5A-B), suggesting that SMAD3 directly interacts with FoxO3 as well as SBEs within the FRE-SBE motif of the proximal promoter region. Overexpression of wtFoxO3, and to a lesser extent, wtSMAD3, independently increased FoxO3 binding within the wt reporter (Figure 3.5C). In the SBE-mut reporter, wtFoxO3 overexpression, but not wtSMAD3 overexpression increased FoxO3-DNA binding (Figure 3.5D). Co-expression of wtFoxO3 and wtSMAD3 increased FoxO3 binding to DNA to a greater extent than overexpression of FoxO3 alone in both the wt and SBE-mut reporters (Figure 3.5C-D).

**Overexpression of SMAD3 increases FoxO3 expression and transcriptional activity**

As indicated above, overexpression of dnSMAD3, which lacks the DNA binding region, was insufficient to induce *MuRF-1* promoter activity, suggesting SMAD3-induced *MuRF-1* gene transcription is dependent on DNA binding. However, wtSMAD3 overexpression was sufficient to induce *MuRF-1* promoter activity in the SBE-mut 0.25kb MuRF-1 reporter (c.f. Figure 3.4) despite the fact that SMAD binding to the FRE-SBE motif was completely abolished in the SBE-mut reporter (c.f. Figure 3.5B).

Together these data suggest SMAD3-induced MuRF-1 promoter activity is dependent of DNA binding at sites outside of the *MuRF-1* promoter region. We therefore hypothesized that SMAD3-induced *MuRF-1* promoter activity may be mediated by increased FoxO expression. In order to determine the effects of SMAD3 on FoxO3 expression, we infected C2C12 myotubes with increasing dosages of ad-wtSMAD3 and analyzed FoxO3 expression by Western blot. As shown in Figure 3.6A, wtSMAD3 overexpression increased FoxO3 expression in a dose-dependent manner. Immunoblots of HEK cells transfected with wtSMAD3 revealed similar results (images not shown). However, wtSMAD3 overexpression was insufficient to induce FoxO1 or FoxO3 gene transcription (Figure 3.6B).

In order to determine whether SMAD3-induced increases in FoxO protein content affect global FoxO-dependent gene transcription, we co-transfected 293a HEK cells with plasmid DNA encoding an FRE reporter and wtFoxO1, wtFoxO3, and/or wtSMAD3. As shown in Figure 3.6C, both wtFoxO1 and wtFoxO3 independently increased FRE-luciferase activity. Interestingly, although wtSMAD3 alone was insufficient to induce FRE-luciferase activity (1.29 fold, $p=0.14$), co-expression of wtFoxO1+wtSMAD3 or FoxO3+SMAD3 increased FRE-luciferase activity to a greater extent than wtFoxO1 or wtFoxO3 alone.

**Discussion:**

The major finding of this study is that SMAD3 synergistically augments FoxO-induced transcription of muscle-specific ubiquitin ligases *Atrogin-1* and *MuRF-1* by increasing FoxO binding to DNA at FRE-SBE motifs within the promoter region of these genes. While a few studies have found these transcription factors coordinately regulate gene expression (2, 33, 89), to our knowledge this is the first study to demonstrate a synergistic effect of these transcription factors on transcription of E3 ubiquitin ligases. Our data indicate that two major pathways (IGF-1-Akt-FoxO pathway and TGF-β signaling) regulating skeletal muscle mass converge to synergistically upregulate genes involved in UPS-mediated protein degradation.

Both FoxO and SMAD transcription factors are known to increase protein degradation (56, 83, 85, 107). FoxO transcription factors are known to upregulate transcription of both *Atrogin-1* (83) and *MuRF-1* (100) by binding the FRE within the promoter regions of these genes, but the role of SMAD3 is less clear. Sartori (85) and Goodman (35) showed that SMAD3 was sufficient to induce expression of *Atrogin-1* and induce muscle atrophy, but was insufficient to induce *MuRF-1* gene transcription. Our data confirm that SMAD3 overexpression is insufficient to induce 5kb *MuRF-1* promoter activity or *MuRF-1* gene expression, but demonstrate that SMAD3 augments FoxO-induced gene expression of *Atrogin-1* and *MuRF-1*. Genetic knockdown of FoxO (81, 87, 93) or SMAD (30, 38) prevents muscle atrophy in numerous chronic conditions. Since both Atrogin-1 and MuRF-1 are required for muscle atrophy (8), it is possible that disrupting the synergistic effects of FoxO and SMAD3 may preserve muscle mass during cachectic conditions by preventing upregulation of these ubiquitin ligases.

Furthermore, we have demonstrated that SMAD3 binding to the FRE-SBE motif is essential for optimal FoxO-induced *MuRF-1* gene transcription. Overexpression of a dnSMAD3 or a SBE-mut MuRF-1 reporter significantly attenuated FoxO-induced MuRF-1 promoter activity (cf Figure 3.4). Additionally, we demonstrated that FoxO3-DNA binding was dramatically reduced in the SBE-mut reporter (cf Figure 3.5C-D). Interestingly, SMAD3-DNA binding increases with co-expression of FoxO3 and SMAD3, even in the SBE-mut reporter (see Figure 5A-B), indicating that SMAD3 directly interacts with FoxO3. These data suggest that FoxO and SMAD3 colocalize at FRE-SBE motifs thus increasing stability of both transcription factors at these sites and augmenting each other's transcriptional activity. This presents a model where SMAD3 directly interacts with both FoxO3 and DNA at the FRE-SBE motif to stabilize FoxO3 DNA interaction thereby augmenting FoxO3-induced gene transcription. It has previously been shown that FoxO and SMAD transcription factors physically associate (89) and FREs and SBEs lie within close proximity within promoter regions of genes coordinately regulated by FoxO and SMAD3 (33). Therefore, it is possible that disrupting SMAD3-DNA interactions may attenuate FoxO-dependent gene transcription by decreasing FoxO3 affinity for FREs. Future studies should systematically test whether SMAD3 inhibition is sufficient to inhibit FoxO-induced transcription of ubiquitin ligases and prevent muscle atrophy.

In contrast to our data, Lokireddy et al. (56) demonstrated that myostatin administration increased UPS-mediated protein degradation in a SMAD3-dependent manner, but SMAD3 knockdown had no effect on myostatin-induced *MuRF-1* gene expression. It is well known that myostatin activates SMAD2 and SMAD3 (99).

Therefore, it is possible that SMAD2 and 3 have redundant roles in regulating *MuRF-1* gene expression. Perhaps with knockdown of both of these transcription factors, these researchers may have seen a decrease in myostatin-induced *MuRF-1* gene expression. In addition to augmenting FoxO-induced MuRF-1 gene transcription, we demonstrated that SMAD3 increases FoxO protein content and global FoxO-induced transcriptional activity. Protein content of FoxO1 and FoxO3 has been shown to increase following myostatin administration in HSkMC myotubes (57), and SMAD3 inhibition may prevent this effect. However, the exact mechanism of this effect is not known. It has previously been suggested that SMAD3 directly induces gene transcription of FoxO1 (57). However, in the present study, we found no differences in FoxO1 or FoxO3 gene expression following SMAD3 overexpression in C2C12 myotubes, suggesting SMAD3 increases FoxO protein content by inhibiting degradation of FoxO proteins. In addition to increased protein content, SMAD3 decreases Akt-mediated phosphorylation (inhibition) of FoxO (4, 67, 99). Increased protein content and decreased phosphorylation of FoxO would be expected to increase global FoxO-dependent transcriptional activity. Using a FRE-reporter, we found that SMAD3 augmented FoxO1 and FoxO3-dependent gene transcription, although SMAD3 overexpression alone was insufficient to induce FRE-luciferase activity.

In our analysis of the *Atrogin-1* and *MuRF-1* promoter regions, we noted the FRE-SBE motif occurs frequently in the proximal promoter region of both genes. In the mouse genome we noted three such motifs within the proximal 1.5kb of the *Atrogin-1* promoter region and two motifs within the proximal 1.5kb of the *MuRF-1* promoter region. The additional FRE-SBE motif in the Atrogin-1 gene may explain why we saw a

greater effect of SMAD3-FoxO3 co-expression on *Atrogin-1* gene expression. In addition to *Atrogin-1* and *MuRF-1*, FoxO3 is known to regulate expression of several genes involved in the autophagic/lysosomal pathway (107). It is possible that similar motifs are located within the promoter regions of these genes and that SMAD3 may directly regulate FoxO-dependent transcription of these genes. Future studies should aim to determine other protein degradation genes that are coordinately regulated by FoxO and SMAD3 within skeletal muscle. Additionally, SMAD3 may augment the transcriptional activity of other DNA binding factors that regulate muscle mass such as the glucocorticoid receptor and nuclear factor-Kβ (NF-Kβ). It should be noted that our work primarily focused on the proximal 0.25kb of the *MuRF-1* promoter region. This region, as well and the FRE-SBE motif, are highly conserved between the mouse and human genomes, indicating the physiological significance of this work in humans.

In summary, our data indicate that SMAD3 synergistically increases, and is essential for, FoxO-induced transcription of ubiquitin ligases through dual mechanisms (Figure 3.7). SMAD3 increases FoxO protein content and directly interacts with DNA at the FRE-SBE motif within the proximal promoter region and stabilizes FoxO binding to enhance its transcriptional activity. These data indicate that two major transcription factors regulating protein degradation converge at the proximal promoter region to induce gene transcription of MuRF-1.

## Tables and Figures

| Gene | | Sequence (5'-3') |
|---|---|---|
| FoxO1 | Fwd | ACCCTGAAGTGCTCGACATC |
| | Rev | TGCTGTGAAGGGACAGATTG |
| FoxO3 | Fwd | GAGTGGATGGTGAAGAGCGT |
| | Rev | CTTCATTCTGAACGCGCA |
| Atrogin-1 | Fwd | TCAGGGATGTGAGCTGTGAC |
| | Rev | GACTGGACTTCTCGACTGCC |
| MuRF-1 | Fwd | TGCAGCGGATCACGCAGGAG |
| | Rev | TGCAGCGGATCACGCAGGAG |
| RPLPO | Fwd | GGCACTTGAGAGGAAGGTAGCCC |
| | Rev | CCGATCTGCAGACACACACT |

| Gene | | Sequence (5'-3') |
|---|---|---|
| Atrogin-1 | Fwd | TCAGGGATGTGAGCTGTGAC |
| | Rev | GGGGGAAGCTTTCAACAGAC |
| MuRF-1 | Fwd | CTTCGTGCTCCTTGCACAT |
| | Rev | ATCGTCACGGAGTGTACGG |
| RPLPO | Fwd | AGGCGTCCTCGTGGAAGTGACA |
| | Rev | TGCTGCATCTGCTTGGAGCCC |

**Table 3.1. Primers used for RT-PCR.** Top panel: sequences for the mouse genome. Bottom panel: sequences for the human genome.

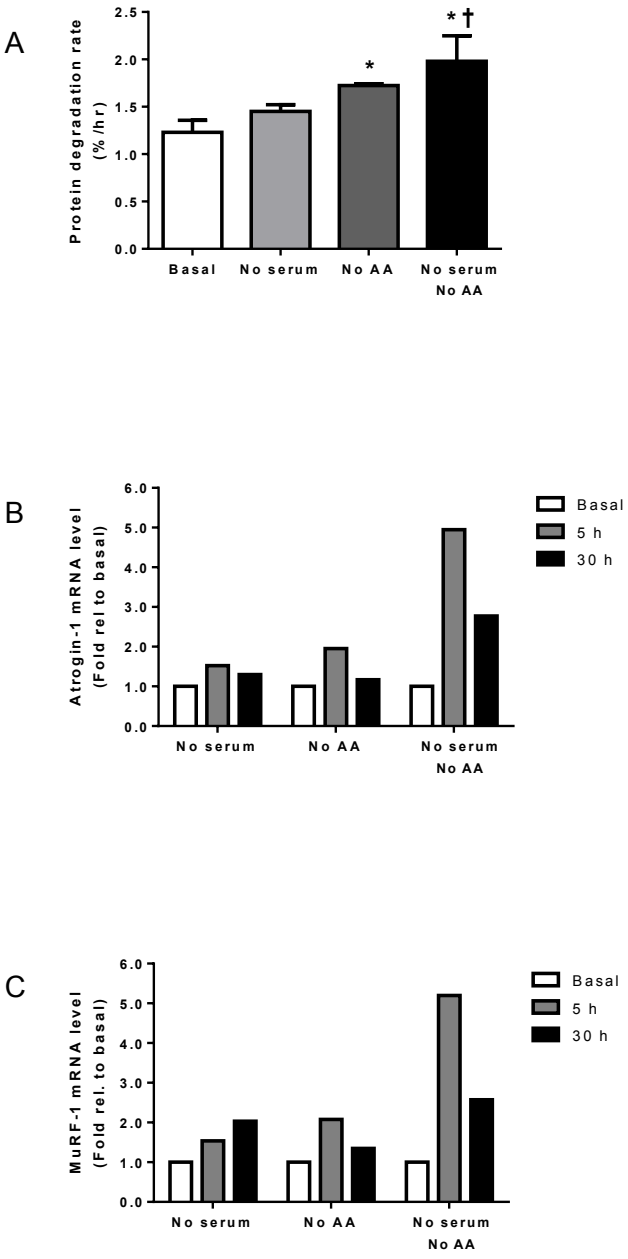


**Figure 3.1. Atrophy stimulation increases protein degradation rate and ubiquitin ligase gene expression in HSkMC myotubes.** Pooled myotubes (from four individuals) were cultured in media lacking serum, lacking amino acids, or lacking both serum and amino acids. A: Protein degradation rate was determined by $^{3}$H-tyrosine release over the course of 5 h. Data are presented as mean ± SEM. * Significantly different from basal ($p<0.05$). † Significantly different from serum-starved ($p<0.05$). B: Atrogin-1 gene expression. C: MuRF-1 gene expression.

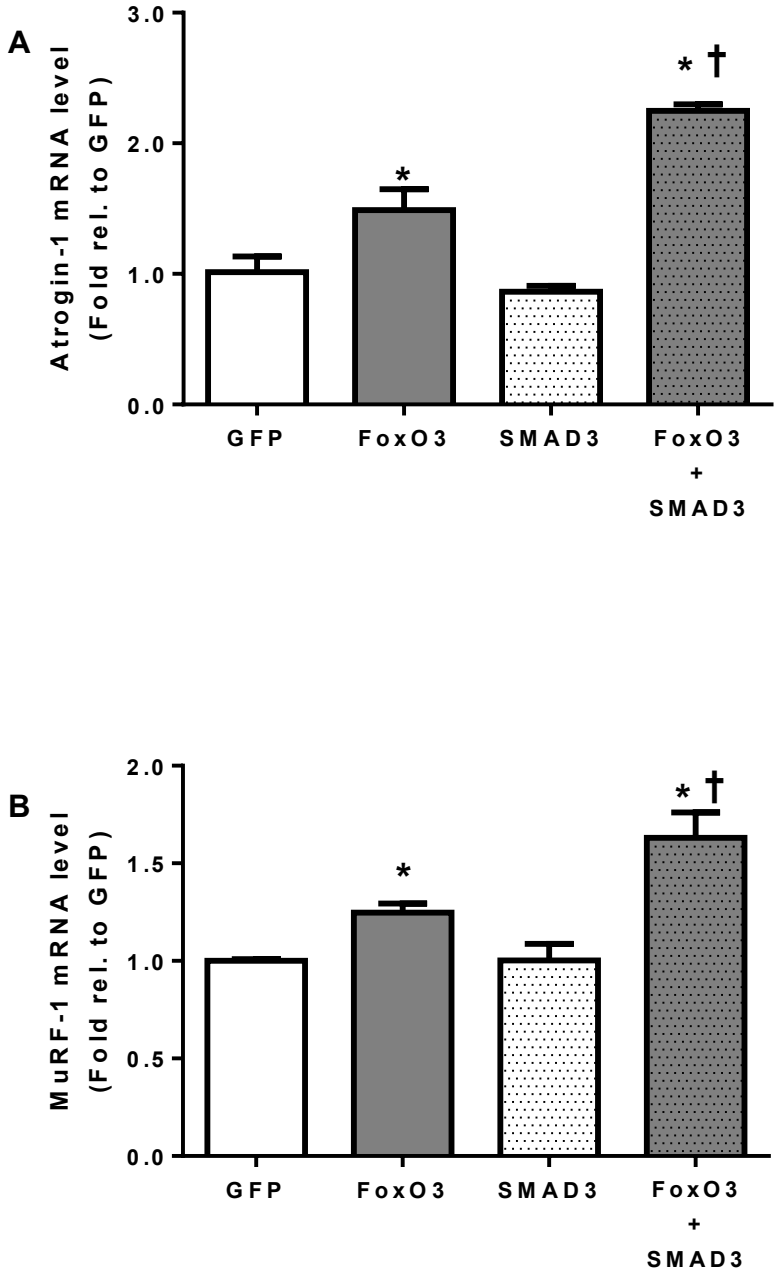


**Figure 3.2. FoxO3 and SMAD3 synergistically activate ubiquitin ligase gene transcription.** C2C12 myotubes were infected with adenoviruses encoding wtSMAD3 and/or wtFoxO3, RNA collected, and RT-PCR performed. A: Atrogin-1 gene expression. B: MuRF-1 gene expression. Data are presented as mean ± SEM. * Significantly different from basal ($p<0.05$). † Significantly different from respective FoxO overexpression only ($p<0.05$).

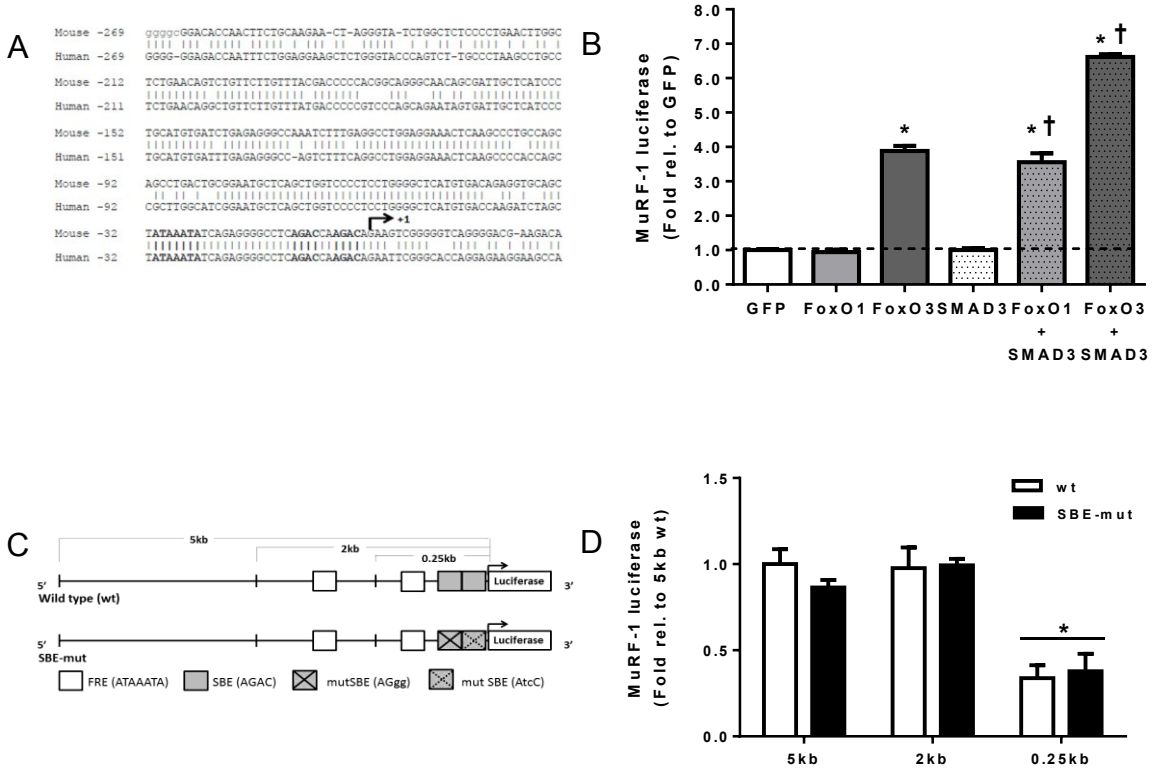


**Figure 3.3. The proximal 0.25kb of the *MuRF-1* promoter is highly conserved and accounts for over one-third of basal transcriptional activity.** A: The 0.25kb reporter sequence is highly conserved between human and mouse genomes FoxO Response Element (FRE) and SMAD Binding Elements (SBE) of the FRE-SBE motif appear in bold. B: Human Embryonic Kidney (HEK293a) cells were transfected with plasmid DNA encoding a 5kb MuRF-1 reporter, SMAD3, wtFoxO1, and/or wtFoxO3. Protein was collected following 48 h of transfection and luciferase activity was measured. * Significantly different from basal ($p<0.05$). † Significantly different from respective FoxO overexpression only ($p<0.05$). C: Schematic diagram of reporters used in the current study. D: Basal luciferase activity of the reporters used. Data are presented as mean ± SEM. * Significantly different from 5kb wt.

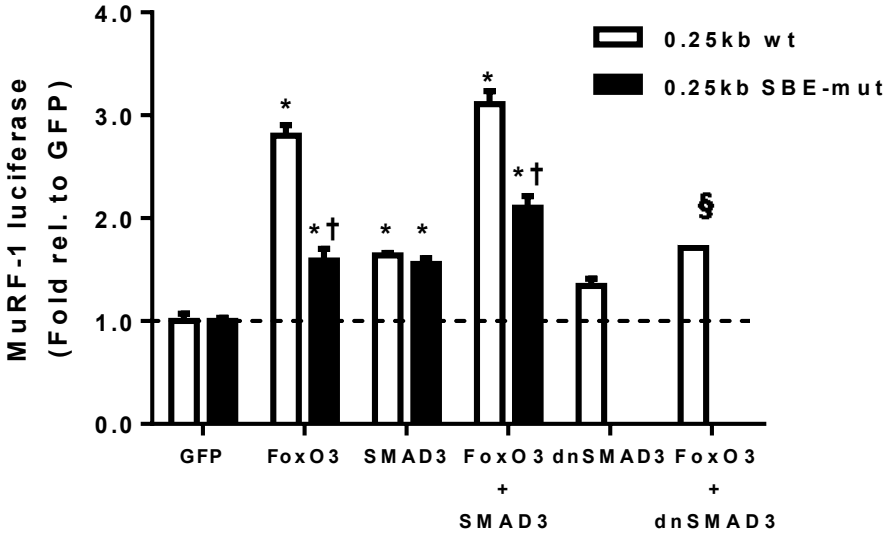


**Figure 3.4. SMAD3 enhances FoxO3-induced *MuRF-1* promoter activity in a DNA binding dependent manner.** HEK 293a cells were transfected with plasmid DNA encoding a 0.25kb (wt or SBE-mut) MuRF-1 reporter, wtFoxO3, wtSMAD3, and/or dnSMAD3. Data are presented as mean ± SEM. * Significantly different from basal ($p<0.05$). † Significantly different from wt ($p<0.05$). § Significantly different from FoxO3 alone.

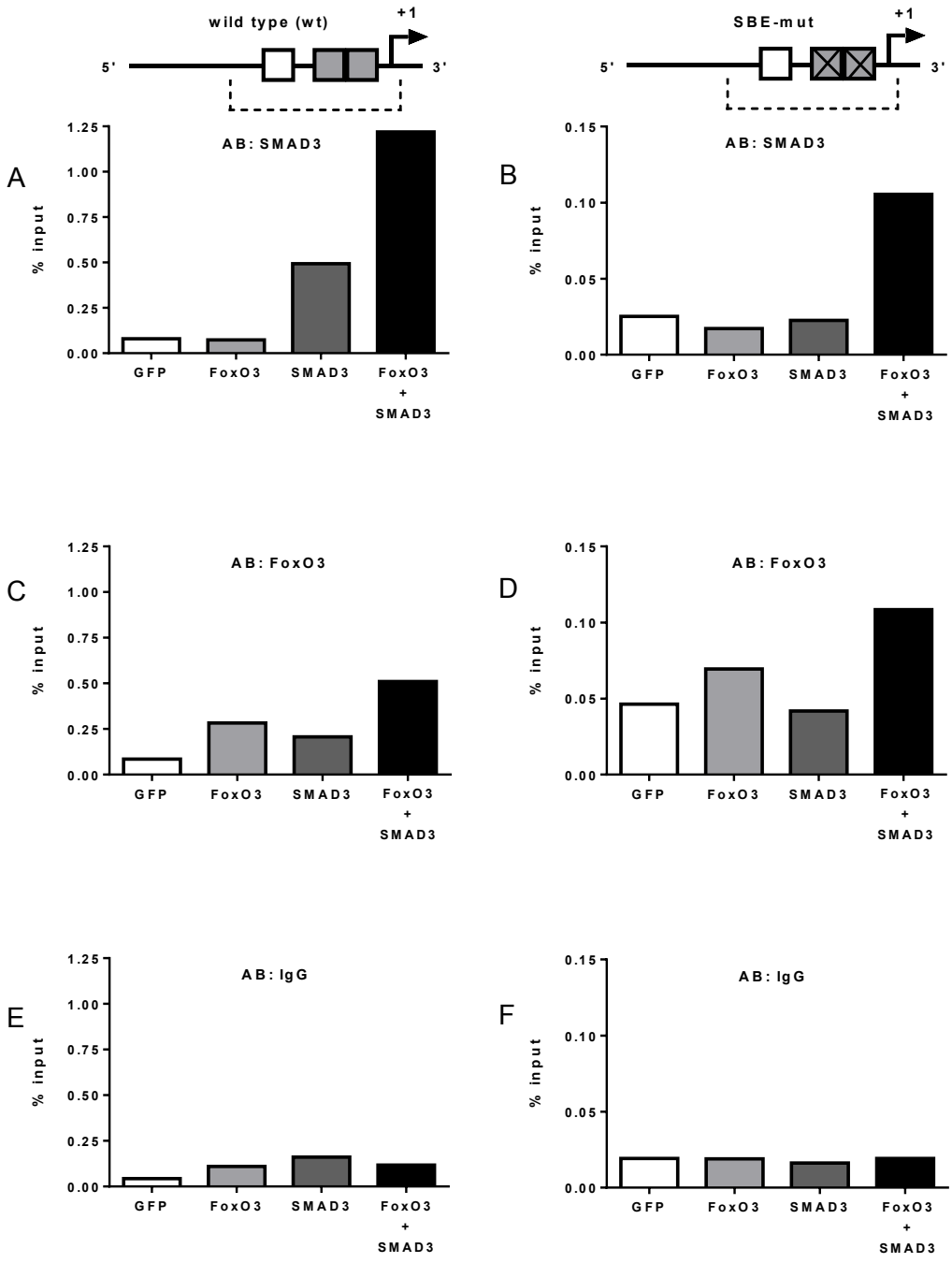


**Figure 3.5. SMAD3 augments FoxO3 binding within the proximal *MuRF-1* promoter region.** Human Embryonic Kidney (HEK293a) cells were transfected with plasmid DNA encoding the 0.25kb MuRF-1 reporter (wt or SBE-mut), wtSMAD3 and/or wtFoxO and chromatin immunoprecipitation performed. A-B: SMAD3 binding to the wt and SBE-mut reporters. C-D: FoxO3 binding to the wt and SBE-mut reporters. E-F: IgG (control antibody) binding to the wt and SBE-mut reporters.

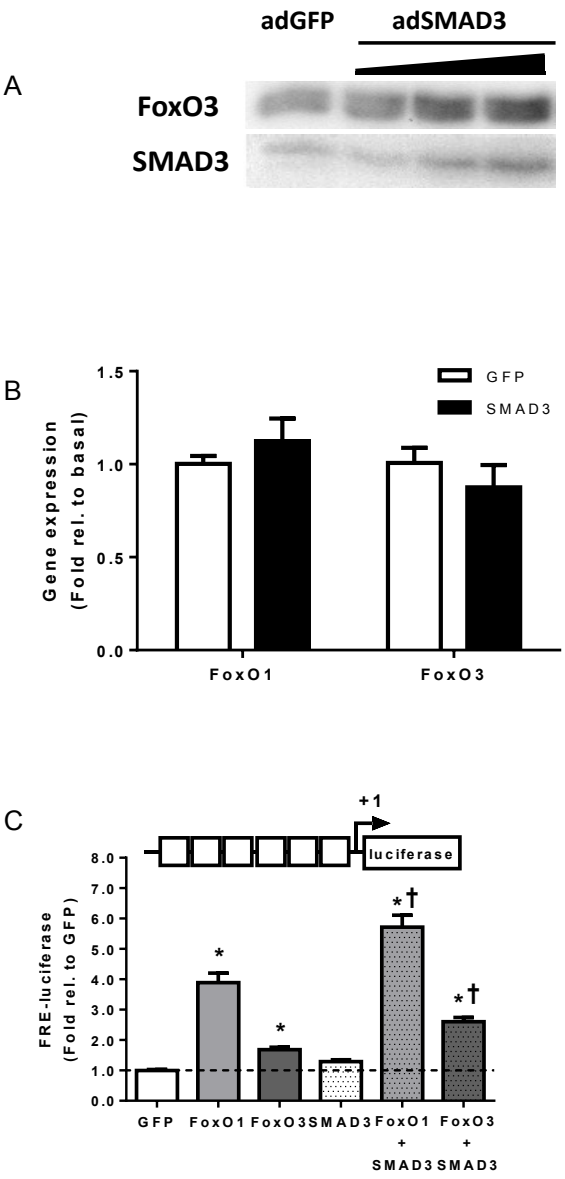


**Figure 3.6. SMAD3 overexpression increases expression and transcriptional activity of FoxO3.** A: C2C12 myotubes were infected with increasing dosages of adenovirus encoding wtSMAD for 24 h, protein collected, and Western blot performed for FoxO3. B: Human Embryonic Kidney (HEK293a) cells were transfected with plasmid DNA encoding a FoxO Response Element (FRE) luciferase reporter, wtSMAD3, wtFoxO1, and/or wtFoxO3. Protein was collected following 48 h of transfection and luciferase activity measured. * Significantly different from basal ($p<0.05$). † Significantly different from FoxO alone ($p<0.05$).

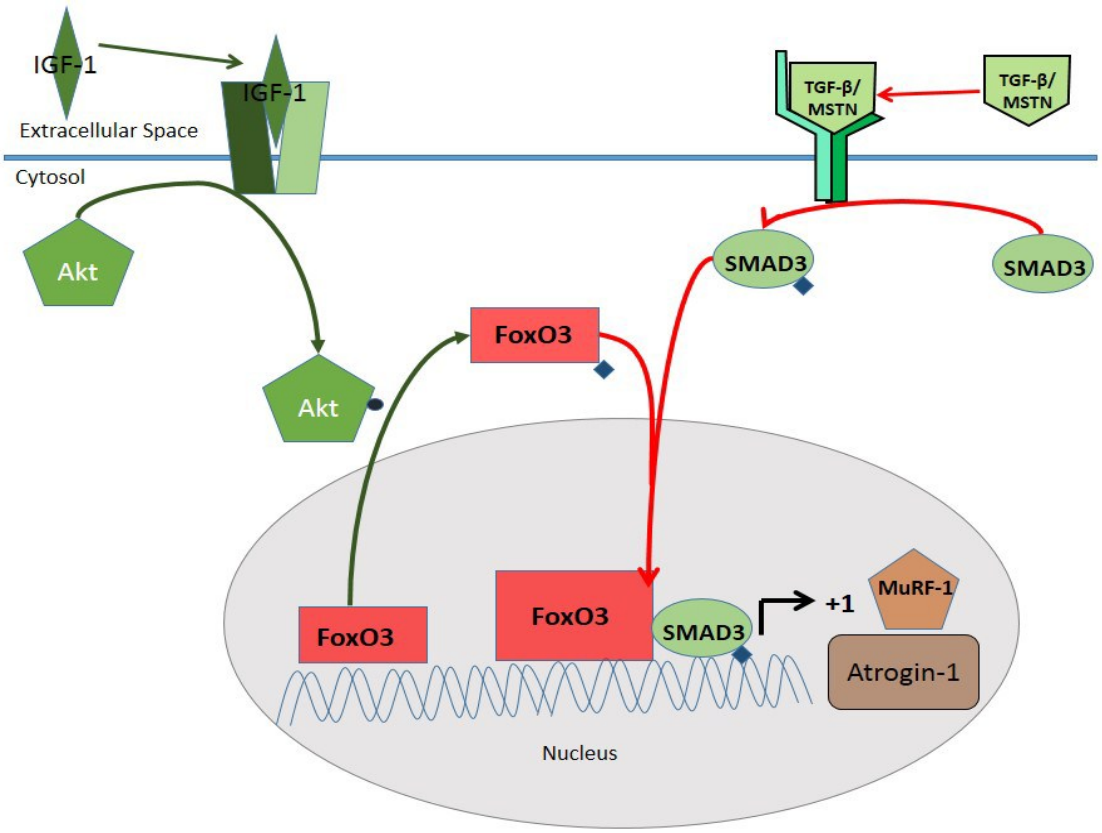


**Figure 3.7. Proposed dualistic mechanism of SMAD3 regulating FoxO3-induced MuRF-1 transcription.** Cytosolic SMAD3 is phosphorylated by the Activin receptor complex upon ligand binding. Phosphorylated SMAD3 forms a transcriptionally active complex with SMAD4 (not shown) and gains nuclear access. SMAD3 binding to the FRE-SBE motif stabilizes FoxO3 binding within the proximal MuRF-1 promoter region to enhance FoxO-dependent gene transcription. Additionally, SMAD3 increases FoxO3 protein content, and in turn, transcriptional activity. The combination of these pathways provides a feed-forward mechanism to upregulate MuRF-1 during muscle atrophy. TGF-β: Transforming Growth Factor-β. MSTN: myostatin

# Chapter 4: Supplementary data

## Rationale

Obesity is accompanied by increased skeletal muscle mass (27, 69), fiber diameter (28), and strength (53). Myocellular size is dictated by the balance between protein synthesis and degradation rates (34). Therefore, the apparent hypertrophic phenotype observed in obesity must be due to differences between protein synthesis and/or degradation rates. Using HSkMC, a cell culture model that retains many characteristics of obesity *in vitro* (43), we found no differences in protein synthesis or degradation rates between lean and severely obese (c.f. Figure 2.2, Supporting information 2.2). Numerous factors affecting protein synthesis and degradation, such as muscular overload and nutritional status/cellular milleu are different between lean and obese *in vivo*. To determine whether excess adipose tissue may provide a training stimulus to increase muscle mass in obesity, we correlated lean body mass and fat mass in lean and obese women using dual-energy x-ray absorptiometry. Additionally, in order to determine whether increased circulating free fatty acids may increase skeletal muscle mass, we incubated C2C12 myotubes in a high lipid environment for up to 72 h and measured protein synthesis and degradation rates.

## Methods

### DEXA scans

Dual-energy x-ray absorptiometery (DEXA) scans from 29 lean (BMI 18.5-24.9) and 50 obese (BMI ≥ 30.0, including 32 post-gastric bypass patients) women were analyzed for mineral-free lean mass and fat mass. Subject characteristics can be found in Table 4.1. Scans were previously collected through ongoing studies at East Carolina University under IRB approval. In order to retain anonymity of subjects, no personal identifiers were retained during these analyses. Regions of interest were drawn by bisecting the glenohumeral joint (arms) or the neck of the femur (leg) to calculate lean mass and fat mass of these appendages. In cases of extreme obesity, hemi-scans were performed and body composition calculated by doubling values obtained from hemi-scans.

### Cell culture

Mouse skeletal muscle myoblasts (C2C12) were cultured in DMEM supplemented with 10% fetal bovine serum and 1% penicillin/streptomycin and maintained at sub-confluent density prior to differentiation. For all experiments, myoblasts were seeded into six well plates at a density of $2.5x10^5$ cells per well and allowed to adhere to the plate overnight. Growth media was switched to low serum media (2% horse serum) to induce differentiation into myotubes. All cell cultures were maintained at 37°C and 5% $CO_2$ and media was changed every 48 h. Following terminal differentiation myotubes were cultured in media supplemented with 500μM lipid (1:1 Palmitate:Oleate) and 1mM L-

Carnitine as a transport protein for up to 72 h. To make 500μM lipid, 0.5 ml Palmitate (200mM) was dissolved in 6.7 ml warm 30% BSA. Once dissolved, 11.8 ml of warm differential media was added. Once in solution, 1 ml of 100mM Oleate was added (20mM) stock. Stock lipid was diluted to a final concentration of 500μM. For all experiments, control, 24 h, 48 h, and 72 h lipid treated myotubes were tested on the same day of differentiation.

**Real-time PCR**

Myotubes were washed twice with PBS, then cells were dissolved in 1 ml TRIzol (Ambion) and nucleotides were allowed to dissociate at room temperature for 10 min. Chloroform (0.2 ml) was added and tubes rotated end-over-end for 10 min then centrifuged at 12,000 x g for 12 min and the supernatant added to 0.5 ml isopropanol. RNA was pelleted by centrifugation (12,000 x g for 8 min), washed with 1.5 ml 70% ethanol, dissolved in 0.05 ml TE buffer and dissociated at 58°C for 10 min. RNA was stored at -80°C until processing. RNA integrity was determined by agarose gel electrophoresis. RNA concentration and purity (Ab260/280) was assessed spectrophometrically using a NanoDrop UV-Vis spectrophometer (ThermoScientific, ND-1000). RNA was reversed transcribed to cDNA (Quanta Biosciences) at a final concentration of 0.10 μg/μl. Fold expression of was calculated using the ΔΔCt method. The geometric mean of Large Ribosomal Protein (RPLPO), GAPDH, and β-actin was used as an endogenous control. Custom RT-PCR primers (Table 4.2) were generated using NCBI BLAST algorithms (http://blast.ncbi.nlm.nih.gov/Blast.cgi) and specificity

confirmed by agarose gel electrophoresis following conventional PCR. All RT-PCR experiments were run with a standard curve of eight orders of magnitude and amplification efficiency determined to be near 100%.

**Luciferase assay**

C2C12 myoblasts were plated in six-well plates at a density of $2.5x10^5$ cells per well and allowed to adhere overnight. Myoblasts were transfected with plasmid DNA encoding a 6x SBE firefly luciferase reporter and a control pRL-Thymidine Kinase control reporter using Fugene 6 per manufacturer's recommendations (Promega). Myotubes were switched to low serum media to induce differentiation and treated with lipid as described above. Myotubes were washed twice with PBS and collected in 1x passive lysis buffer per manufacturer's recommendation (Promega). Samples were spun at 20,000 x g for 5 min and 20 µl of the supernatant pipetted into a white 96-well plate with 100 µl of substrate. Luminescence was measured using a microplate reader (Spectramax M4). Firefly luciferase (SBE reporter) was normalized to that of the control RL-Tk reporter and values were expressed as fold difference relative to untreated.

**Protein synthesis**

Lipid treated C2C12 myotubes were radiolabeled with L-[3,5-$^3$H] tyrosine (5 µCi/ml, PerkinElmer Life Sciences) for 2 h, residual radioactivity was washed away, and proteins were precipitated with 10% TCA. Proteins were collected in microcentrifuge

tubes, pelleted by centrifugation, and then dissolved in 0.1N NaOH. Radioactivity incorporation was determined by scintillation counting and normalized to total protein content as assessed by bicinchoninic acid (BCA) assay (ThermoScientific).

**Protein degradation assay**

Protein degradation rate was determined by release of a radiolabeled amino acid as previously described (11, 107). Terminally differentiated myotubes were radiolabeled with L-[3,5-$^{3}$H] tyrosine (5 μCi/ml, PerkinElmer Life Sciences) for 24 h. Cells were thoroughly washed and radioactivity chased for 2 h using differentiation media supplemented with 2 mM L-tyrosine to allow degradation of short-lived proteins and to limit re-incorporation of the radiolabel. Four serial media samples were collected over the course of 5 h. At the end of the experiments, culture media was removed completely and myotubes were solubilized in 0.2N NaOH. Radioactivity of cells and TCA-precipitated media samples was measured using scintillation counting. Total radioactivity was calculated as the sum of the residual radioactivity in the myotubes plus radioactivity of all time points. Protein degradation rate was directly calculated as a percentage of total [$^{3}$H] tyrosine incorporation from the regression line of serial samples for each individual.

## Tables and Figures

| | n | age | ht (m) | wt (kg) | BMI (kg/m2) |
|---|---|---|---|---|---|
| Lean | 29 | 43.3 ± 3.7 | 1.66 ± 0.01 | 62.8 ± 1.00 | 22.8 ± 0.3 |
| Obese | 50 | 46.2 ± 1.7 | 1.57 ± 0.01 | 101.8 ± 2.80* | 41.6 ± 1.3* |

**Table 4.1. Subject Characteristics.** Data are presented as mean ± SEM. * $p < 0.05$ vs. lean.

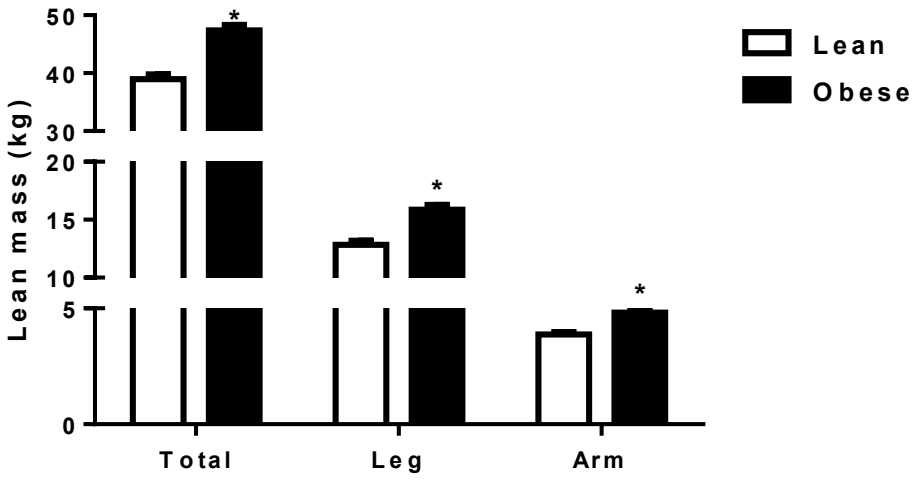


**Figure 4.1. Lean body mass is increased in obesity.** Dual-energy x-ray absorptiometry (DEXA) scans from 29 lean and 50 obese women were analyzed for lean body mass and fat mass. Regions of interest were determined by bisecting the glenohumeral joint (arm) or the neck of the femur (leg). Data are presented as mean ± SEM. *$p<0.05$ lean vs obese.

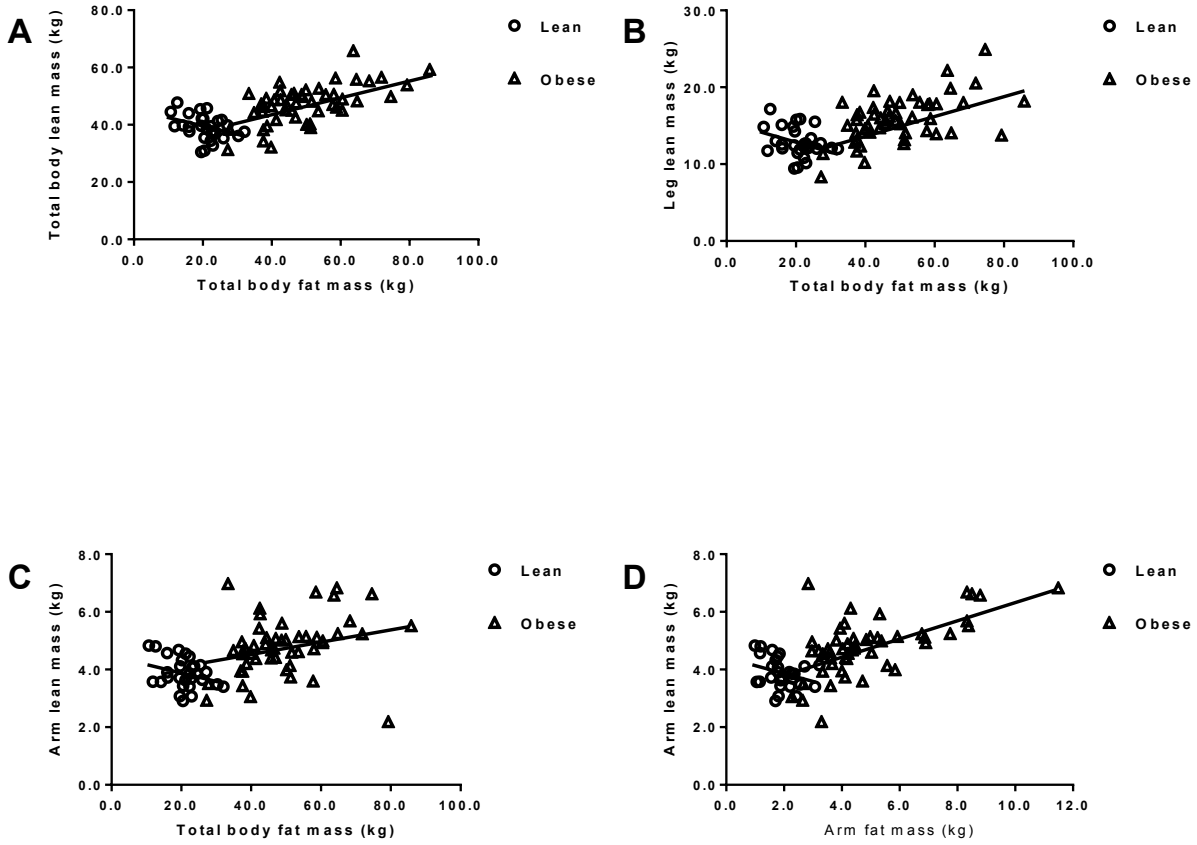


**Figure 4.2. Fat mass predicts lean body mass in obesity.** A: Total body fat mass predicts total lean body mass in both lean ($r=-0.379$, $p<0.05$) and obese ($r=0.606$, $p<0.0001$) women. B: Total body fat mass predicts lean mass of the legs in obese ($r=0.537$, $p<0.0001$), but not lean ($r=-0.274$, $p=0.15$), women. C: Total body fat mass predicts lean mass of the arms in obese ($r=0.286$, $p<0.05$), but not lean ($r=-0.341$, $p=0.07$). D: Fat mass of the arms predicts lean mass of the arms in obese ($r=0.618$, $p<0.0001$), but not lean ($r=-0.332$, $p=0.08$).

| Pathway | Gene | | Sequence (5'-3') |
|---|---|---|---|
| TGF-β signaling | **ACVRIB** | **Fwd** | TTGGTCTGTAGGCAGCTGGT |
| | | **Rev** | TTCTTCCCCCTTGTTGTCCT |
| | **SMAD2** | **Fwd** | TTTGCTGTACTCAGTCCCCA |
| | | **Rev** | TGAGCTTGAGAAAGCCATCA |
| | **SMAD3** | **Fwd** | ACAGGCGGCAGTAGATAACG |
| | | **Rev** | CGTAATTCATGGTGGCTGTG |
| | **SMAD4** | **Fwd** | GGCTCTCCTTCAAAGTCGTG |
| | | **Rev** | GGTTGTCTCACCTGGAATTGA |
| | **SMAD7** | **Fwd** | CTTCTCCTCCCAGTATGCCA |
| | | **Rev** | GAACGAATTATCTGGCCCCT |
| Autophagic/lysosomal pathway genes | **LC3B** | **Fwd** | AATCACTGGCATCTTGGTGG |
| | | **Rev** | GAGAAGACCTTCAAGCAGCG |
| | **ATG4B** | **Fwd** | TTTCTGCCCAGAATCCAAAC |
| | | **Rev** | TCGGACAGGGAAGATGGA |
| | **Gabarapl-1** | **Fwd** | TAGGAGCCTTCTCCACGATG |
| | | **Rev** | AGGACCACCCCTTCGAGTAT |
| | **BECN1** | **Fwd** | GGCGAGTTTCAATAAATGGC |
| | | **Rev** | CCAGGAACTCAGCTCCAT |
| Ubiquitin-proteasome system genes | **FoxO3** | **Fwd** | CTTCATTCTGAACGCGCA |
| | | **Rev** | CTTCAAGGATAAGGGCGACA |
| | **Atrogin-1** | **Fwd** | TCAGGGATGTGAGCTGTGAC |
| | | **Rev** | GACTGGACTTCTCGACTGCC |
| | **MuRF-1** | **Fwd** | TGCAGCGGATCACGCAGGAG |
| | | **Rev** | TGGCACTTGAGAGGAAGGTAGCCC |
| Control genes | **RPLPO** | **Fwd** | CCGATCTGCAGACACACACT |
| | | **Rev** | ACCCTGAAGTGCTCGACATC |
| | **B-actin** | **Fwd** | GCTGTATTCCCCTCCATCGTG |
| | | **Rev** | CACGGTTGGCCTTAGGGTTCAG |
| | **GAPDH** | **Fwd** | ACCCAGAAGACTGTGGATGG |
| | | **Rev** | CACATTGGGGTAGGAACAC |

**Table 4.2. Primers used for RT-PCR.**

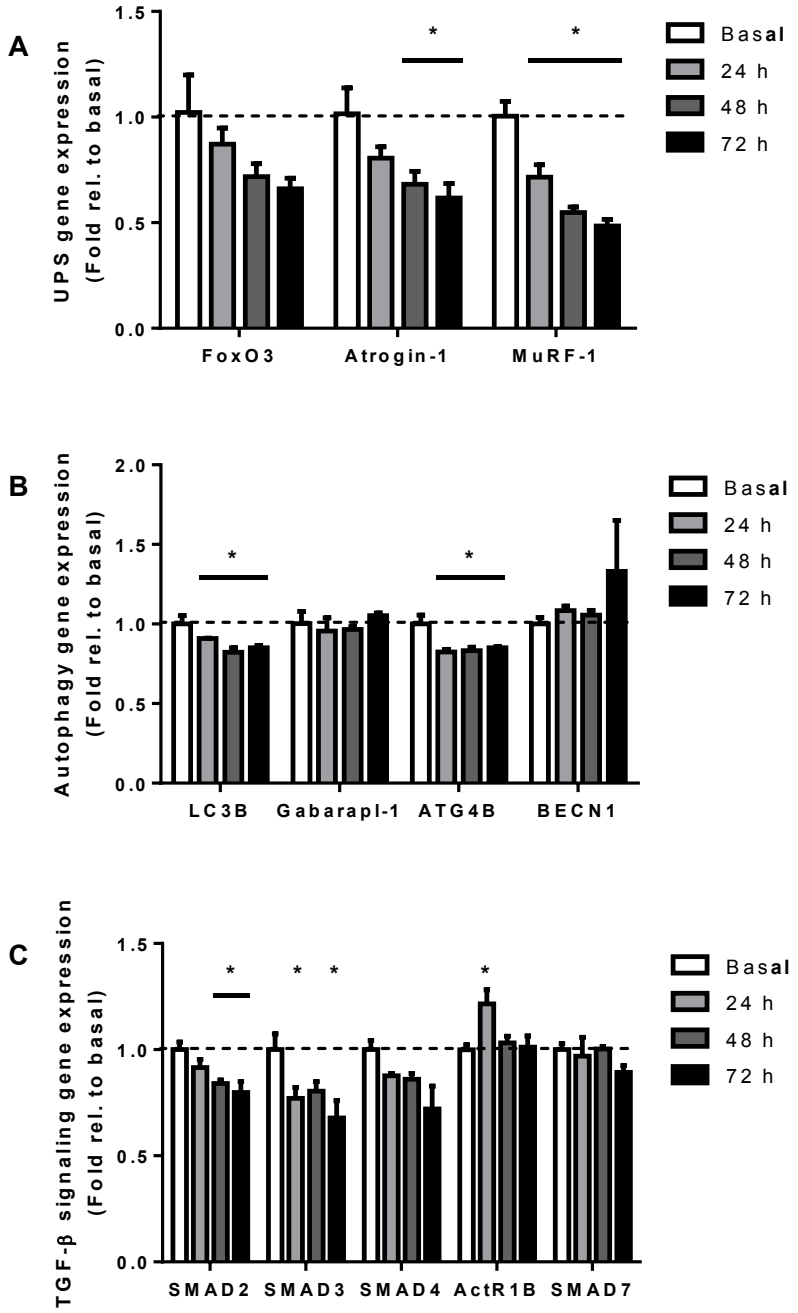


**Figure 4.3. Lipid exposure decreases expression of genes involved in protein degradation.** C2C12 myotubes were cultured in media containing 500μM Palmitate:Oleate for up to 72 h. A: genes involved in the ubiquitin-proteasome system. B: genes involved in the autophagic/lysosomal pathway. C: genes involved in TGF-β signaling. Data are presented as mean ± SEM. * $p<0.05$ vs basal

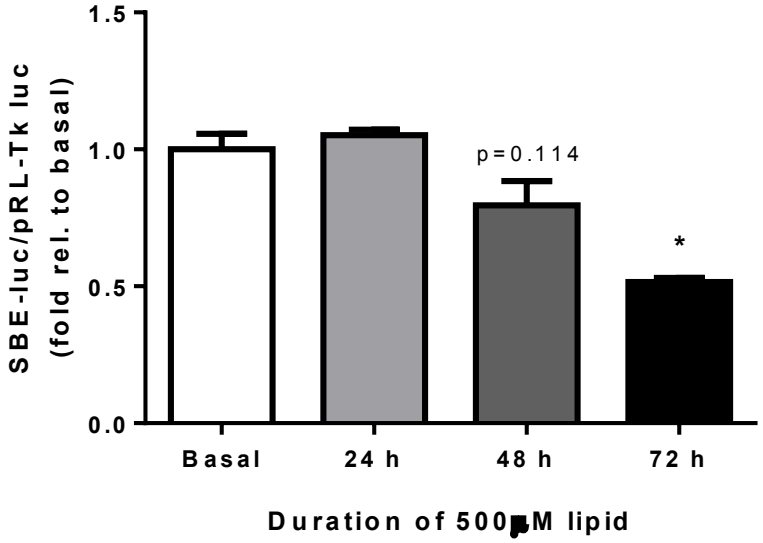


**Figure 4.4. Prolonged lipid exposure decreases SMAD-dependent gene transcription.** Myoblasts were transfected with plasmid DNA encoding a 6xSBE reporter and a control renilla reporter. Terminally differentiated myotubes were cultured in media containing 500µM Palmitate:Oleate for up to 72 h. SBE-luciferase activity was normalized to RL-Tk activity to control for transfection efficiency. Data are presented as mean ± SEM. *p<0.05 vs basal.

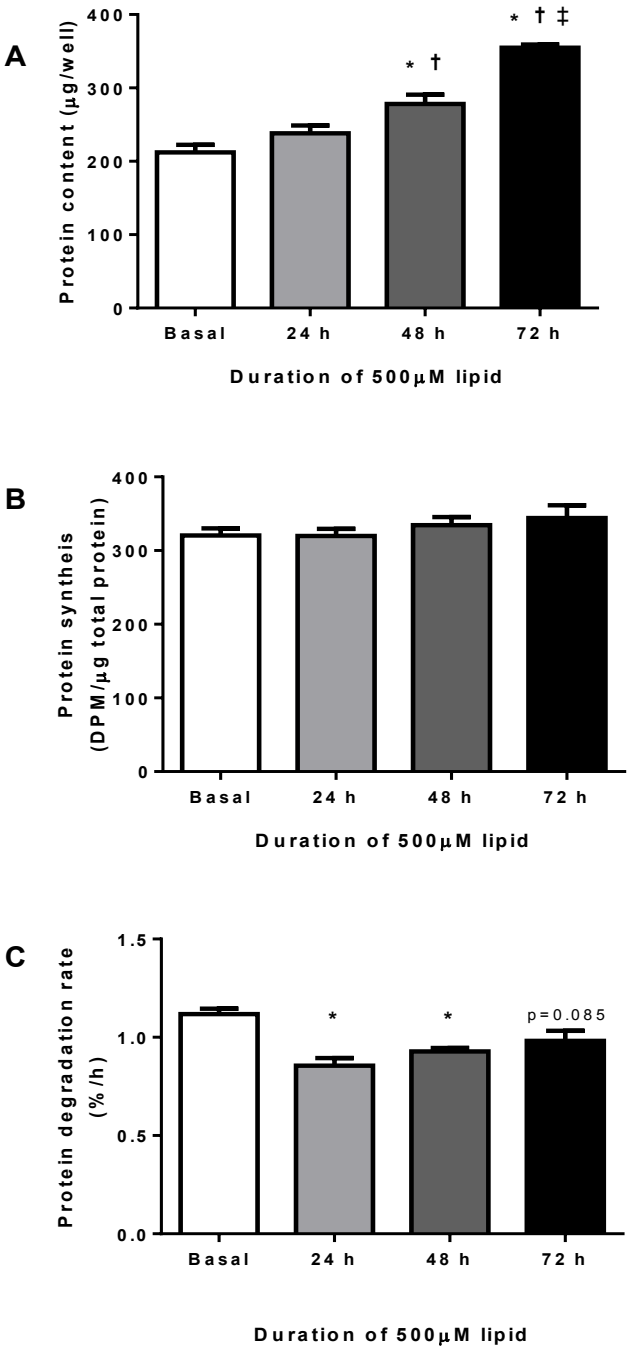


**Figure 4.5. Exposure to high fat increases total protein content in C2C12 myotubes by decreasing basal protein synthesis rate.** Terminally differentiated myotubes were cultured in media containing 500µM Palmitate:Oleate for up to 72 h. A: Protein content B: Protein synthesis rate measured over 2 h by 3H-tyrosine incorporation. C:Protein degradation rate measured by 3H-tyrosine release over the course of 5 h. Data are presented as mean ± SEM. * $p<0.05$ vs basal. † $p<0.05$ vs 24 h. ‡ $p<0.05$ vs 48h.

## Chapter 5: Global discussion

Due to the common transcriptional response shared between numerous forms of muscle atrophy (13, 54, 82) and the impaired metabolic profile noted in skeletal muscle of the obese (43), the present project aimed to understand the effects of obesity on the transcriptional regulation of muscle protein degradation. Severe obesity is often accompanied by insulin resistance (50, 77), and subsequently, decreased Akt activity (6). Since Akt is a major regulator of FoxO activity (93), we hypothesized that protein degradation rates would be increased in myotubes of the extremely obese both basally and in response to atrophic stimuli. In order to test this hypothesis, we measured gene expression, flux through the major protein degradation pathways, and myotube area, in primary HSkMC myotubes. This model retains many characteristics of obesity, such as insulin resistance (6), impaired fatty acid oxidation (43), and overexpression of atrophy-related genes (42, 72) but eliminates confounders of in vivo research such as nutrition, circulating amino acid concentrations, hormonal milieu, and muscle overload that can be significantly different between lean and obese. In addition to insulin resistance, skeletal muscle of the severely obese overexpresses myostatin (1), a TGF-β family member that signals through SMAD3 (56, 108). Therefore, we further hypothesized that SMAD3 overexpression would augment FoxO3-induced transcription of genes involved in protein degradation. We directly measured gene expression and promoter activity of MuRF-1, a muscle-specific E3 ubiqutin ligase in response to SMAD3 and FoxO3 overexpression.

**Increased FoxO3 expression does not increase gene expression of FoxO-inducible genes in the severely obese**

Numerous forms of muscle atrophy share a common transcriptional response to increase the rate of protein degradation (13, 54, 82). Therefore, we measured gene expression patterns of protein degradation-related genes in myotubes from lean and severely obese (c.f. Figure 2.1). Gene expression patterns of protein degradation genes of the UPS (*Atrogin-1* and *MuRF-1*) and autophagic/lysosomal pathways (*LC3B*, *Gabarapl-1*, and *ATG4B*) were similar between myotubes of the lean and severely obese under basal and starved conditions. In contrast to previous studies (1, 42, 72), we found no differences in myostatin gene expression in myotubes of the severely obese. Interestingly, gene expression of the transcription factor *FoxO3* was significantly higher in myotubes from the severely obese. FoxO3 induces transcription of genes involved in both the UPS and the autophagic/lysosomal pathway (107). Notably, FoxO3 binds the proximal promoter regions and induces gene expression of *Atrogin-1* (83) and *MuRF-1* (100), two E3 ubiquitin ligases that are essential for muscle atrophy (8). Since *FoxO3* gene expression was increased in myotubes of the severely obese, it would be predicted that gene expression of *Atrogin-1* and *MuRF-1* would also be higher. However, we found no differences in gene expression of the FoxO3-inducible genes *Atrogin-1*, *MuRF-1*, *LC3B*, or *Gabarapl-1* between myotubes of the lean and severely obese.

Waddell et al. (100) recently reported that the glucocorticoid receptor acts to synergistically increase FoxO1-induced MuRF-1 gene transcription. Therefore, it is possible that increased FoxO3 expression alone is insufficient to induce expression of downstream genes involved in protein degradation. Recently, a subset of genes have been shown to be coordinately regulated by FoxO and SMAD transcription factors (2, 33, 89). Therefore, we hypothesized that coordinately overexpressing FoxO3 and SMAD3 may synergistically increase expression of genes involved in protein degradation. Given our finding of increased FoxO3 gene expression and the well-described increase in myostatin (1, 15, 42) and SMAD3 (101) signaling in skeletal muscle of the severely obese *in vivo*, the synergistic effects of these transcription factors may have profound physiological relevance with regard to transcriptional regulation of protein degradation, especially in obesity.

**SMAD3 augments FoxO3-induced transcription of ubiquitin ligases**

Both FoxO3 (83, 107) and SMAD3 (35, 56, 57, 85) have been shown to independently increase protein degradation and cause muscle atrophy *in vitro* and *in vivo*. In order to determine whether SMAD3 augments FoxO3-induced transcription of protein degradation genes, we co-expressed these transcription factors in C2C12 myotubes and measured gene expression (c.f. Figure 3.2). As expected, overexpression of wtFoxO3 independently increased gene expression of both *Atrogin-1* and *MuRF-1*. Overexpression of wtSMAD3 was insufficient to significantly increase gene expression of either *Atrogin-1* or *MuRF-1*. Interestingly, co-expression of FoxO3

and SMAD3 synergistically increased gene expression of both *Atrogin-1* and *MuRF-1*, indicating SMAD3 and FoxO3 synergistically regulate expression of ubiquitin ligases essential for protein degradation and muscle atrophy. Contrary to previous studies (42, 72), we found no difference in myostatin expression between myotubes of the lean and severely obese. The absence of increased signaling through this pathway may explain the similar expression patterns of *Atrogin-1* and *MuRF-1* and protein degradation rates between myotubes of the lean and severely obese under basal conditions. During numerous forms of muscle atrophy, signaling through the TGF-β pathway is increased (13, 19, 29, 60, 102). We subjected myotubes to both starvation and dexamethasone to induce protein degradation. Both of these treatments decreased myostatin and SMAD3 gene expression. Given the increased FoxO3 gene expression in skeletal muscle of the severely obese, atrophic stimuli that increase signaling through this pathway may cause dramatically increased ubiquitin ligase gene expression and UPS-mediated protein degradation.

According to our data, SMAD3 augments FoxO3-induced MuRF-1 gene transcription via dual mechanisms: 1) increasing FoxO3 content and 2) augmenting FoxO3 binding to DNA within the proximal MuRF-1 promoter region (c.f. Figure 3.7). We discovered a highly conserved FRE-SBE motif within the proximal MuRF-1 promoter region (c.f. Figure 3.3A). Interestingly, three similar motifs were noted in the proximal 1.5 kb of the mouse *Atrogin-1* promoter region. This may explain why we observed a greater induction of *Atrogin-1* gene expression in response to FoxO3 and SMAD3 co-expression. Aligning the mouse and human *Atrogin-1* promoter regions revealed these FRE-SBE motifs are not conserved within the human genome.

However, we did note one FRE-SBE motif within the proximal promoter region of *Atrogin-1* in the human genome indicating this mechanism likely regulates *Atrogin-1* gene transcription as well. Gomis et al. (33) previously reported that FRE and SBE occur within close proximity of 11 genes coordinately regulated by FoxO and SMAD3 transcription factors, but found no consensus sequence. Therefore, it is possible that FoxO and SMAD3 coordinately regulate expression of other ubiquitin ligases, and potentially, genes involved in the autophagic/lysosomal pathway.

**Flux through the major protein degradation pathways is altered in skeletal muscle of the severely obese**

Contrary to our original hypothesis, we found no difference in total protein degradation rates although flux (c.f. Figure 2.2) through the ubiquitin-proteasome system (UPS) and autophagic/lysosomal protein degradation pathways were significantly different between myotubes from the lean and severely obese (cf Figure 2.3). Compared to lean, the rate of flux through the autophagic/lysosomal pathway was significantly lower in myotubes of the severely obese under basal and starved conditions. Impaired flux through the autophagic/lysosomal pathway via muscle-specific knockout of Atg7 results in impaired mitochondrial structure and function, increased ROS production, and insulin resistance in mice (106). It is possible that decreased flux through this pathway may explain several metabolic abnormalities seen in obesity such as insulin resistance and impaired mitochondrial function both *in vitro* and *in vivo*. While we did not examine these variables in the present study, future research should aim to

determine the cellular mechanism of autophagy deficiency-induced insulin resistance and its physiological significance *in vivo*.

Additionally, in response to starvation, myotubes of the severely obese displayed a shift toward UPS-mediated protein degradation. The differential contribution of protein degradation pathways in response to starvation suggests that specific proteins degraded during atrophy may be different between lean and the severely obese. For example, contractile proteins of the thick filament are ubiquitinated by MuRF-1 and subsequently degraded by the UPS (18). Recently, Atrogin-1 has been shown to directly interact with components of the intermediate filament as well as contractile proteins (58). While we did not observe any differences in myotube area between lean and obese during starvation, it is possible that during muscle atrophy, the shift toward UPS-mediated protein degradation results in a greater loss of contractile proteins, and therefore, muscle strength in the severely obese. Restoring flux through the major protein degradation pathways may preserve skeletal muscle metabolism and contractile function and thus abrogate some of the negative health consequences of obesity.

Coordinate increases in FoxO3 expression and SMAD3 signaling may contribute to the increased UPS flux seen during starvation in myotubes of the severely obese. It is well-described that myostatin expression (42, 59, 72) and SMAD3 phosphorylation (101) is increased in skeletal muscle of the obese in vivo. Sishi et al. (91) noted increased MuRF-1 protein content in skeletal muscle of obese, prediabetic rats which may be explained by increased FoxO3 and SMAD3 acting on the proximal promoter region. While we did not observe any differences in gene FoxO3 or SMAD3 gene

expression between myotubes of the lean and severely obese, both of these transcription factors undergo post-translational phosphorylation to modulate activity. FoxO3 activity is directly inhibited by Akt-mediated phosphorylation (93). Given the insulin resistance noted in our subjects, we can postulate that FoxO3 activity would be higher in our severely obese myotubes since this phenotype is retained *in vitro*. Increased FoxO activity in the obese would be expected to augment residual SMAD3 activity, resulting in increased ubiquitin ligase gene transcription. While we did not observe any differences in *Atrogin-1* and *MuRF-1* gene expression between myotubes of the lean and severely obese, many genes involved in protein degradation are directly regulated by FoxO3 (107). It is possible that the FRE-SBE motif is present in the promoter regions of other genes involved in protein degradation.

**Proteasome activity is higher in skeletal muscle of the severely obese**

Flux through the UPS is dependent not only on polyubiquitination of proteins, but also on proteasome subunit composition and, subsequently, proteasome activity. We noted that proteasome capacity was higher in myotubes from the severely obese compared to those of lean (c.f. Figure 2.4). Hwang et al. (45) previously reported differential proteasome subunit composition between skeletal muscles of the lean and overweight diabetics. Additionally, numerous proteins are known to associate with and regulate proteolytic activity of the proteasome (21, 76). It has previously been shown that expression of these genes is altered during aging-induced muscle atrophy (3). It is possible that promoter regions of the genes are also affected by FoxO3 and SMAD3 in

a similar manner. This mechanism may explain the increased proteasome capacity noted in myotubes of the severely obese.

**Mechanisms of muscular hypertrophy in obesity**

Myocellular size is dictated by the balance between rates of protein synthesis and degradation (34). Previous reports in animals (74, 92) and humans (75) have shown blunted protein synthesis rates in obesity. To date, studies regarding protein degradation in obesity have yielded controversial results. Diet-induced obesity increases expression of genes involved in protein degradation such as myostatin (59) and MuRF-1 (91). Protein degradation at the whole-body level is increased in obesity (39, 103). Meanwhile, skeletal muscle protein degradation is decreased in obesity (73). However, observational data have consistently shown that obesity is accompanied by increased strength (53), skeletal muscle mass (27, 69), and increased fiber diameter (28) compared to lean.

Our HSkMC myotube data indicates that protein synthesis and degradation rates are not inherently different between skeletal muscle of the lean and severely obese. Therefore, it is possible that other factors such as increased muscular overload or cellular environment in obesity contribute to increased muscle mass.

**Excess adipose tissue may contribute to increased muscle mass in obesity by increasing muscular overload**

In order to determine whether increased muscular overload due to excess adiposity alters muscle mass in obesity, we analyzed dual-energy absorptiometry (DEXA) scans from 29 lean (BMI 18.5-24.9) and 50 obese (BMI>30.0) women. As expected, mineral-free lean body mass, a surrogate of muscle mass (12, 41), was higher in the obese (Figure 4.1). In order to determine whether adiposity per se increases muscle mass by increasing muscle overload, we also analyzed lean body mass of the load-bearing (legs) and non-load-bearing appendages (arms). Lean body mass of the legs and arms was significantly higher in the obese (Figure 4.1). Interestingly, total lean body mass was negatively correlated with total body fat mass in the lean (-0.379), but positively correlated with total body fat mass in the obese (0.606) (Figure 4.2A). Additionally, lean body mass of the load-bearing appendages was positively correlated with total body fat mass in the obese (0.537), but not the lean (Figure 4.2B). A weak correlation was noted between lean body mass of the non-load-bearing appendages and total body fat mass in the obese (0.286), but not the lean (Figure 4.2C). Interestingly, we found that a strong correlation between lean body mass of the non-load-bearing appendages and fat mass of the non-load-bearing appendages in the obese (0.618) (Figure 4.2D). Together, these data suggest that increased fat mass may result in muscular hypertrophy by increasing muscular overload and providing a training stimulus *in vivo* as has been previously hypothesized (44). However, the magnitude of this effect on basal protein synthesis and degradation rates

may be difficult to measure *in vivo* and thus contribute to the disparate protein degradation results of previous studies.

**High fat exposure increases myocellular size by decreasing protein degradation rate**

In addition to adiposity, obesity is accompanied by increased circulating fatty acids (7). Therefore, in order determine how a high fat cellular environment affects transcriptional regulation of protein degradation, we incubated C2C12 myotubes in media containing high fatty acids for up to 72 h. High fat exposure significantly decreased, expression of genes involved in the UPS, autophagic/lysosomal pathway, and TGF-β signaling. Notably, gene expression of *Atrogin-1* and *MuRF-1* was significantly down-regulated in response to high fat exposure (Figure 4.3A). A similar pattern of gene expression was noted for FoxO3, although this trend failed to reach statistical significance. Expression of genes involved in the autophagic/lysosomal pathway was more variable in their response to high fat exposure. Gene expression of both LC3B and ATG4B were significantly down-regulated in response to high fat exposure (Figure 4.3B). However, both Gabarapl-1 and BECN1 were unaffected by high fat exposure. Interestingly, genes involved in TGF-β signaling were significantly down-regulated in response to high fat exposure. Gene expression of both SMAD2 and SMAD3 gene expression was significantly decreased in response to high fat exposure (Figure 4.3C). This pathway has recently been implicated in the development of skeletal muscle insulin resistance (96) and signaling through this pathway is increased

in obesity (59, 101). High fat exposure induces marked insulin resistance *in vitro* (6). Downregulation of TGF-β signaling may serve to maintain insulin sensitivity during this treatment.

To determine whether decreased expression of TGF-β signaling genes alters transcriptional response to this pathway, we expressed a SBE-luciferase plasmid in C2C12 and measured basal luciferase activity in response to high fat exposure. SBE-luciferase activity was unchanged following 24 h of high fat exposure, but decreased in a step-wise manner with prolonged exposure to high fat (Figure 4.4). Our data show that SMAD3 is a crucial regulator of FoxO3-induced *Atrogin-1* and *MuRF-1* gene expression. In fact, knockdown of SMAD3 transcriptional activity significantly attenuated FoxO3-induced *MuRF-1* promoter activity. Therefore, it is possible that decreased SMAD transcriptional activity may drive the decreased *Atrogin-1* and *MuRF-1* gene expression noted with prolonged high fat exposure.

Interestingly, prolonged exposure to high fat significantly increased protein content of C2C12 myotubes (Figure 4.5A) and this effect was independent of protein synthesis (Figure 4.5B). Exposure to high fat for 24 h significantly attenuated basal protein degradation rate in C2C12 myotubes and this persisted through 48 h of high fat exposure (Figure 4.5C). Therefore, it is possible that acute exposure to high fat, such as following a high fat meal or increased lipolytic activity, may reduce skeletal muscle protein degradation rate. Interestingly, prolonged high fat exposure increased protein degradation rate in a step-wise manner; following 72 h of high fat exposure, protein degradation rate was not significantly different from basal. Therefore, chronic high fat

exposure may produce compensatory mechanisms to increase basal protein degradation rate. Since circulating free fatty acid concentration is higher in the obese (7, 94), this may explain why basal protein degradation rates are similar between skeletal muscles of the lean and severely obese. Furthermore, repeated transient increases in high fat exposure, such as following multiple high fat meals, may produce transient post-prandial decreases in protein degradation which may in turn contribute to increased skeletal muscle mass observed in obesity.

Taken together, the current project indicates that the transcriptional regulation of protein degradation is not inherently different between skeletal muscles of the lean and severely obese. Despite the similar transcriptional regulation of protein degradation, myotubes of the severely obese have decreased flux through the autophagic/lysosomal pathway which may contribute to impaired mitochondrial function and insulin resistance both *in vitro* and *in vivo*. In myotubes of the severely obese, starvation induces a shift toward UPS-mediated protein degradation which may result in increased degradation of sarcomeric proteins and, ultimately, decreased force production. FoxO3, a major transcriptional regulator of both UPS and autophagic/lysosomal-mediated protein degradation, is overexpressed in myotubes of the severely obese. Furthermore, FoxO3 is synergistically activated by SMAD3 via dual mechanisms: 1) increased FoxO3 protein content and 2) increased FoxO3 binding at conserved FRE-SBE motifs within the promoter region of FoxO3-inducible genes. Coordinate activation of both these transcription factors likely contributes to upregulation of ubiquitin ligases during muscle atrophy. Given our finding of increased *FoxO3* gene expression in skeletal muscle of the severely obese, it is possible that atrophic stimuli that increase TGF-β signaling may

cause dramatically increased protein degradation and muscle atrophy in the severely obese. Furthermore, exposure of myotubes to an obesogenic environment decreases expression of protein degradation genes and transiently decreases protein degradation rates. Repeated exposure to this type of environment, combined with increased daily loading from increased adiposity may contribute to the increased skeletal muscle mass seen in obesity.

## References


1. **Allen DL, Cleary AS, Speaker KJ, Lindsay SF, Uyenishi J, Reed JM, Madden MC, Mehan RS**. Myostatin, activin receptor IIb, and follistatin-like-3 gene expression are altered in adipose tissue and skeletal muscle of obese mice. *Am. J. Physiol. Endocrinol. Metab.* 294: E918–27, 2008.

2. **Allen DL, Unterman TG**. Regulation of myostatin expression and myoblast differentiation by FoxO and SMAD transcription factors. *Am. J. Physiol. Cell Physiol.* 292: 188–99, 2007.

3. **Altun M, Besche HC, Overkleeft HS, Piccirillo R, Edelmann MJ, Kessler BM, Goldberg AL, Ulfhake B**. Muscle wasting in aged, sarcopenic rats is associated with enhanced activity of the ubiquitin proteasome pathway. *J. Biol. Chem.* 285: 39597–608, 2010.

4. **Amirouche A, Durieux A-C, Banzet S, Koulmann N, Bonnefoy R, Mouret C, Bigard X, Peinnequin A, Freyssenet D**. Down-regulation of Akt/mammalian target of rapamycin signaling pathway in response to myostatin overexpression in skeletal muscle. *Endocrinology* 150: 286–94, 2009.

5. **Berggren JR, Tanner CJ, Houmard JA**. Primary cell cultures in the study of human muscle metabolism. *Exerc. Sport Sci. Rev.* 35: 56–61, 2007.

6. **Bikman BT, Zheng D, Reed MA, Hickner RC, Houmard JA, Dohm GL**. Lipid-induced insulin resistance is prevented in lean and obese myotubes by AICAR treatment. *Am. J. Physiol. Regul. Integr. Comp. Physiol.* 298: R1692–9, 2010.

7. **Björntorp P, Bergman H, Varnauskas E**. Plasma free fatty acid turnover rate in obesity. *Acta Med. Scand.* 185: 351–6, 1969.

8. **Bodine SC, Latres E, Baumhueter S, Lai VK, Nunez L, Clarke BA, Poueymirou WT, Panaro FJ, Na E, Dharmarajan K, Pan ZQ, Valenzuela DM, DeChiara TM, Stitt TN, Yancopoulos GD, Glass DJ**. Identification of ubiquitin ligases required for skeletal muscle atrophy. *Science* 294: 1704–8, 2001.

9. **Bonnard C, Durand A, Peyrol S, Chanseaume E, Chauvin M-A, Morio B, Vidal H, Rieusset J**. Mitochondrial dysfunction results from oxidative stress in the skeletal muscle of diet-induced insulin-resistant mice. *J. Clin. Invest.* 118: 789–800, 2008.

10. **Boyle KE, Zheng D, Anderson EJ, Neufer PD, Houmard JA**. Mitochondrial lipid oxidation is impaired in cultured myotubes from obese humans. *Int. J. Obes.* 36: 1025–31, 2012.

11. **Brault JJ, Jespersen JG, Goldberg AL**. Peroxisome proliferator-activated receptor gamma coactivator 1alpha or 1beta overexpression inhibits muscle protein degradation, induction of ubiquitin ligases, and disuse atrophy. *J. Biol. Chem.* 285: 19460–71, 2010.

12. **Bridge P, Pocock NA, Nguyen T, Munns C, Cowell CT, Thompson MW**. Prediction of appendicular skeletal and fat mass in children: excellent concordance of dual-energy X-ray absorptiometry and magnetic resonance imaging. *J. Pediatr. Endocrinol. Metab.* 22: 795–804, 2009.

13. **Calura E, Cagnin S, Raffaello A, Laveder P, Lanfranchi G, Romualdi C**. Meta-analysis of expression signatures of muscle atrophy: gene interaction networks in early and late stages. *BMC Genomics* 9: 630, 2008.

14. **Carlson CJ, Booth FW, Gordon SE**. Skeletal muscle myostatin mRNA expression is fiber-type specific and increases during hindlimb unloading. *Am. J. Physiol.* 277: R601–6, 1999.

15. **Chen M-J, Han D-S, Yang J-H, Yang Y-S, Ho H-N, Yang W-S**. Myostatin and its association with abdominal obesity, androgen and follistatin levels in women with polycystic ovary syndrome. *Hum. Reprod.* 27: 2476–83, 2012.

16. **Choy L, Skillington J, Derynck R**. Roles of autocrine TGF-beta receptor and Smad signaling in adipocyte differentiation. *J. Cell Biol.* 149: 667–82, 2000.

17. **Clarke B a, Drujan D, Willis MS, Murphy LO, Corpina R a, Burova E, Rakhilin S V, Stitt TN, Patterson C, Latres E, Glass DJ**. The E3 Ligase MuRF1 degrades myosin heavy chain protein in dexamethasone-treated skeletal muscle. *Cell Metab.* 6: 376–85, 2007.

18. **Cohen S, Brault JJ, Gygi SP, Glass DJ, Valenzuela DM, Gartner C, Latres E, Goldberg AL**. During muscle atrophy, thick, but not thin, filament components are degraded by MuRF1-dependent ubiquitylation. *J. Cell Biol.* 185: 1083–95, 2009.

19. **Costelli P, Muscaritoli M, Bonetto a., Penna F, Reffo P, Bossola M, Bonelli G, Doglietto GB, Baccino FM, Fanelli FR**. Muscle myostatin signalling is enhanced in experimental cancer cachexia. *Eur. J. Clin. Invest.* 38: 531–538, 2008.

20. **Csibi A, Leibovitch MP, Cornille K, Tintignac LA, Leibovitch SA**. MAFbx/Atrogin-1 controls the activity of the initiation factor eIF3-f in skeletal muscle atrophy by targeting multiple C-terminal lysines. *J. Biol. Chem.* 284: 4413–21, 2009.

21. **DeMartino GN, Slaughter CA**. The proteasome, a novel protease regulated by multiple mechanisms. *J. Biol. Chem.* 274: 22123–6, 1999.

22. **Etlinger JD, Goldberg AL**. A soluble ATP-dependent proteolytic system responsible for the degradation of abnormal proteins in reticulocytes. *Proc. Natl. Acad. Sci. U. S. A.* 74: 54–8, 1977.

23. **Falk B, Sadres E, Constantini N, Zigel L, Lidor R, Eliakim A**. The association between adiposity and the response to resistance training among pre- and early-pubertal boys. *J. Pediatr. Endocrinol. Metab.* 15: 597–606, 2002.

24. **Felig, Philip, Marliss, Errol, Cahill GF**. Plasma Amino Acid Levels and Insulin Secretion in Obesity. *N. Engl. J. Med.* 281: 811–816, 1969.

25. **Flegal KM, Carroll MD, Ogden CL, Curtin LR**. Prevalence and trends in obesity among US adults , 1999-2008. *J. Am. Med. Assoc.* 303: 235–241, 2010.

26. **Flegal KM, Kit BK, Orpana H, Graubard BI**. Association of all-cause mortality with overweight and obesity using standard body mass index categories: a systematic review and meta-analysis. *JAMA* 309: 71–82, 2013.

27. **Forbes GB**. Lean body mass-body fat interrelationships in humans. *Nutr. Rev.* 45: 225–231, 1987.

28. **Gavin TP, Stallings HW, Zwetsloot K a, Westerkamp LM, Ryan N a, Moore R a, Pofahl WE, Hickner RC**. Lower capillary density but no difference in VEGF expression in obese vs. lean young skeletal muscle in humans. *J. Appl. Physiol.* 98: 315–21, 2005.

29. **George I, Bish LT, Kamalakkannan G, Petrilli CM, Oz MC, Naka Y, Sweeney HL, Maybaum S**. Myostatin activation in patients with advanced heart failure and after mechanical unloading. *Eur. J. Heart Fail.* 12: 444–53, 2010.

30. **Gilson H, Schakman O, Combaret L, Lause P, Grobet L, Attaix D, Ketelslegers JM, Thissen JP**. Myostatin gene deletion prevents glucocorticoid-induced muscle atrophy. *Endocrinology* 148: 452–60, 2007.

31. **Gomes A V, Waddell DS, Siu R, Stein M, Dewey S, Furlow JD, Bodine SC**. Upregulation of proteasome activity in muscle RING finger 1-null mice following denervation. *FASEB J.* 26: 2986–99, 2012.

32. **Gomes LC, Scorrano L**. Mitochondrial morphology in mitophagy and macroautophagy. *Biochim. Biophys. Acta* 1833: 205–12, 2013.

33. **Gomis RR, Alarcón C, He W, Wang Q, Seoane J, Lash A, Massagué J**. A FoxO-Smad synexpression group in human keratinocytes. *Proc. Natl. Acad. Sci. U. S. A.* 103: 12747–52, 2006.

34. **Goodman CA, Mayhew DL, Hornberger TA**. Recent progress toward understanding the molecular mechanisms that regulate skeletal muscle mass. *Cell. Signal.* 23: 1896–906, 2011.

35. **Goodman CA, McNally RM, Hoffmann FM, Hornberger TA**. Smad3 Induces Atrogin-1, Inhibits mTOR and Protein Synthesis, and Promotes Muscle Atrophy In Vivo. *Mol. Endocrinol.* (September 3, 2013). doi: 10.1210/me.2013-1194.

36. **Goodpaster BH**. Mitochondrial deficiency is associated with insulin resistance. *Diabetes* 62: 1032–5, 2013.

37. **Han HQ, Zhou X, Mitch WE, Goldberg AL**. Myostatin/Activin Pathway Antagonism: Molecular Basis and Therapeutic Potential. *Int. J. Biochem. Cell Biol.* (May 27, 2013). doi: 10.1016/j.biocel.2013.05.019.

38. **Heineke J, Auger-Messier M, Xu J, Sargent M, York a., Welle S, Molkentin JD**. Genetic Deletion of Myostatin From the Heart Prevents Skeletal Muscle Atrophy in Heart Failure. *Circulation* 121: 419–425, 2010.

39. **Henderson GC, Nadeau D, Horton ES, Nair KS**. Effects of adiposity and 30 days of caloric restriction upon protein metabolism in moderately vs. severely obese women. *Obesity (Silver Spring).* 18: 1135–42, 2010.

40. **Hershko A, Ciechanover A**. The ubiquitin system. *Annu. Rev. Biochem.* 67: 425–79, 1998.

41. **Heymsfield SB, Smith R, Aulet M, Bensen B, Lichtman S, Wang J, Pierson RN**. Appendicular skeletal muscle mass: measurement by dual-photon absorptiometry. *Am. J. Clin. Nutr.* 52: 214–8, 1990.

42. **Hittel DS, Berggren JR, Shearer J, Boyle K, Houmard J a**. Increased secretion and expression of myostatin in skeletal muscle from extremely obese women. *Diabetes* 58: 30–8, 2009.

43. **Houmard JA, Pories WJ, Dohm GL**. Is there a metabolic program in the skeletal muscle of obese individuals? *J. Obes.* 2011: 250496, 2011.

44. **Hulens M, Vansant G, Lysens R, Claessens AL, Muls E, Brumagne S**. Study of differences in peripheral muscle strength of lean versus obese women: an allometric approach. *Int. J. Obes. Relat. Metab. Disord.* 25: 676–81, 2001.

45. **Hwang H, Bowen BP, Lefort N, Flynn CR, De Filippis EA, Roberts C, Smoke CC, Meyer C, Højlund K, Yi Z, Mandarino LJ**. Proteomics analysis of human skeletal muscle reveals novel abnormalities in obesity and type 2 diabetes. *Diabetes* 59: 33–42, 2010.

46. **Jagoe RT, Goldberg AL**. What do we really know about the ubiquitin-proteasome pathway in muscle atrophy? *Curr. Opin. Clin. Nutr. Metab. Care* 4: 183–90, 2001.

47. **Janssen I**. Influence of sarcopenia on the development of physical disability: the Cardiovascular Health Study. *J. Am. Geriatr. Soc.* 54: 56–62, 2006.

48. **Katsanos CS, Mandarino LJ**. Protein metabolism in human obesity: a shift in focus from whole-body to skeletal muscle. *Obesity.* 19: 469–75, 2011.

49. **Kisselev AF, Goldberg AL**. Monitoring activity and inhibition of 26S proteasomes with fluorogenic peptide substrates. *Methods Enzymol.* 398: 364–78, 2005.

50. **Kolterman OG, Insel J, Saekow M, Olefsky JM**. Mechanisms of insulin resistance in human obesity: evidence for receptor and postreceptor defects. *J. Clin. Invest.* 65: 1272–84, 1980.

51. **Krawiec BJ, Frost RA, Vary TC, Jefferson LS, Lang CH**. Hindlimb casting decreases muscle mass in part by proteasome-dependent proteolysis but independent of protein synthesis. *Am. J. Physiol. Endocrinol. Metab.* 289: E969–80, 2005.

52. **Labbé E, Silvestri C, Hoodless PA, Wrana JL, Attisano L**. Smad2 and Smad3 positively and negatively regulate TGF beta-dependent transcription through the forkhead DNA-binding protein FAST2. [Online]. *Mol. Cell* 2: 109–20, 1998.

53. **Lafortuna CL, Maffiuletti N, Agosti F, Sartorio A**. Gender variations of body composition, muscle strength and power output in morbid obesity. *Int. J. Obes.* 29: 833–841, 2005.

54. **Lecker SH, Jagoe RT, Gilbert A, Gomes M, Baracos V, Bailey J, Price SR, Mitch WE, Goldberg AL**. Multiple types of skeletal muscle atrophy involve a common program of changes in gene expression. *FASEB J.* 18: 39–51, 2004.

55. **Lenk K, Schur R, Linke A, Erbs S, Matsumoto Y, Adams V, Schuler G**. Impact of exercise training on myostatin expression in the myocardium and skeletal muscle in a chronic heart failure model. *Eur. J. Heart Fail.* 11: 342–8, 2009.

56. **Lokireddy S, McFarlane C, Ge X, Zhang H, Sze SK, Sharma M, Kambadur R**. Myostatin induces degradation of sarcomeric proteins through a Smad3 signaling mechanism during skeletal muscle wasting. *Mol. Endocrinol.* 25: 1936–49, 2011.

57. **Lokireddy S, Mouly V, Butler-Browne G, Gluckman PD, Sharma M, Kambadur R, McFarlane C**. Myostatin promotes the wasting of human myoblast cultures through promoting ubiquitin-proteasome pathway-mediated loss of sarcomeric proteins. *Am. J. Physiol. Cell Physiol.* 301: C1316–24, 2011.

58. **Lokireddy S, Wijesoma IW, Sze SK, McFarlane C, Kambadur R, Sharma M**. Identification of atrogin-1-targeted proteins during the myostatin-induced skeletal muscle wasting. *Am. J. Physiol. Cell Physiol.* 303: C512–29, 2012.

59. **Lyons J-A, Haring JS, Biga PR**. Myostatin expression, lymphocyte population, and potential cytokine production correlate with predisposition to high-fat diet induced obesity in mice. *PLoS One* 5: e12928, 2010.

60. **Ma K, Mallidis C, Bhasin S, Mahabadi V, Artaza J, Gonzalez-Cadavid N, Arias J, Salehian B**. Glucocorticoid-induced skeletal muscle atrophy is associated with upregulation of myostatin gene expression. *Am. J. Physiol. Endocrinol. Metab.* 285: E363–71, 2003.

61. **Massagué J, Seoane J, Wotton D**. Smad transcription factors. *Genes Dev.* 19: 2783–810, 2005.

62. **Matthews DR, Hosker JP, Rudenski AS, Naylor BA, Treacher DF, Turner RC**. Homeostasis model assessment: insulin resistance and beta-cell function from fasting plasma glucose and insulin concentrations in man. *Diabetologia* 28: 412–9, 1985.

63. **Menconi M, Gonnella P, Petkova V, Lecker S, Hasselgren P-O**. Dexamethasone and corticosterone induce similar, but not identical, muscle wasting responses in cultured L6 and C2C12 myotubes. *J. Cell. Biochem.* 105: 353–64, 2008.

64. **Metter EJ, Talbot LA, Schrager M, Conwit R**. Skeletal muscle strength as a predictor of all-cause mortality in healthy men. *J. Gerontol.* 57: B359–65, 2002.

65. **Mitch WE, Goldberg AL**. Mechanisms of muscle wasting. The role of the ubiquitin-proteasome pathway. *N. Engl. J. Med.* 335: 1897–905, 1996.

66. **Mizushima N, Levine B, Cuervo AM, Klionsky DJ**. Autophagy fights disease through cellular self-digestion. *Nature* 451: 1069–75, 2008.

67. **Morissette MR, Cook S a, Buranasombati C, Rosenberg M a, Rosenzweig A**. Myostatin inhibits IGF-I-induced myotube hypertrophy through Akt. *Am. J. Physiol. Cell Physiol.* 297: C1124–32, 2009.

68. **Morley JE, Thomas DR, Wilson MG**. Cachexia: pathophysiology and clinical relevance. *Am. J. Clin. Nutr.* 83: 735–743, 2006.

69. **Morse WI, Soeldner JS**. The non-adipose body mass of obese women: evidence of increased muscularity. *Can. Med. Assoc. J.* 90: 723–5, 1964.

70. **Murakami K, Voellmy R, Goldberg AL**. Protein degradation is stimulated by ATP in extracts of Escherichia coli. *J. Biol. Chem.* 254: 8194–200, 1979.

71. **Newman AB, Kupelian V, Visser M, Simonsick EM**. Strength , But Not Muscle Mass , Is Associated With Mortality in the Health , Ag ... *Journals Gerontol.* 61: 72–77, 2006.

72. **Park J-J, Berggren JR, Hulver MW, Houmard JA, Hoffman EP**. GRB14, GPD1, and GDF8 as potential network collaborators in weight loss-induced improvements in insulin action in human skeletal muscle. *Physiol. Genomics* 27: 114–21, 2006.

73. **Patterson BW, Horowitz JF, Wu G, Watford M, Coppack SW, Klein S**. Regional muscle and adipose tissue amino acid metabolism in lean and obese women. *Am. J. Physiol. Endocrinol. Metab.* 282: E931–6, 2002.

74. **Paturi S, Gutta AK, Kakarla SK, Katta A, Arnold EC, Wu M, Rice KM, Blough ER**. Impaired overload-induced hypertrophy in obese Zucker rat slow-twitch skeletal muscle. *J. Appl. Physiol.* 108: 7–13, 2010.

75. **Pescatello LS, Kelsey BK, Price TB, Seip RL, Angelopoulos TJ, Clarkson PM, Gordon PM, Moyna NM, Visich PS, Zoeller RF, Gordish-Dressman HA, Bilbie SM, Thompson PD, Hoffman EP**. The muscle strength and size response to upper arm,

unilateral resistance training among adults who are overweight and obese. *J. Strength Cond. Res.* 21: 307–13, 2007.

76. **Piccirillo R, Demontis F, Perrimon N, Goldberg AL**. Mechanisms of muscle growth and atrophy in mammals and Drosophila. *Dev. Dyn.* (August 29, 2013). doi: 10.1002/dvdy.24036.

77. **RABINOWITZ D, ZIERLER KL**. Forearm metabolism in obesity and its response to intra-arterial insulin. Characterization of insulin resistance and evidence for adaptive hyperinsulinism. *J. Clin. Invest.* 41: 2173–81, 1962.

78. **Raffaello A, Laveder P, Romualdi C, Bean C, Toniolo L, Germinario E, Megighian A, Danieli-Betto D, Reggiani C, Lanfranchi G**. Denervation in murine fast-twitch muscle: short-term physiological changes and temporal expression profiling. *Physiol. Genomics* 25: 60–74, 2006.

79. **Ramaswamy S, Nakamura N, Sansal I, Bergeron L, Sellers WR**. A novel mechanism of gene regulation and tumor suppression by the transcription factor FKHR. *Cancer Cell* 2: 81–91, 2002.

80. **Rantanen T, Harris T, Leveille SG, Visser M, Foley D, Masaki K, Guralnik JM**. Muscle strength and body mass index as long-term predictors of mortality in initially healthy men. *journals Gerontol.* 55: M168–73, 2000.

81. **Reed SA, Sandesara PB, Senf SM, Judge AR**. Inhibition of FoxO transcriptional activity prevents muscle fiber atrophy during cachexia and induces hypertrophy. *FASEB J.* 26: 987–1000, 2012.

82. **Sacheck JM, Hyatt J-PK, Raffaello A, Jagoe RT, Roy RR, Edgerton VR, Lecker SH, Goldberg AL**. Rapid disuse and denervation atrophy involve transcriptional changes similar to those of muscle wasting during systemic diseases. *FASEB J.* 21: 140–55, 2007.

83. **Sandri M, Sandri C, Gilbert A, Skurk C, Calabria E, Picard A, Walsh K, Schiaffino S, Lecker SH, Goldberg AL**. Foxo transcription factors induce the atrophy-related ubiquitin ligase atrogin-1 and cause skeletal muscle atrophy. *Cell* 117: 399–412, 2004.

84. **Sandri M**. Protein breakdown in muscle wasting: Role of autophagy-lysosome and ubiquitin-proteasome. *Int. J. Biochem. Cell Biol.* 45: 2121–9, 2013.

85. **Sartori R, Milan G, Patron M, Mammucari C, Blaauw B, Abraham R, Sandri M**. Smad2 and 3 transcription factors control muscle mass in adulthood. *Am. J. Physiol. Cell Physiol.* 296: 1248–1257, 2009.

86. **Schöneich C, Dremina E, Galeva N, Sharov V**. Apoptosis in differentiating C2C12 muscle cells selectively targets Bcl-2-deficient myotubes. *Apoptosis* (October 16, 2013). doi: 10.1007/s10495-013-0922-7.

87. **Senf SM, Dodd SL, Judge AR**. FOXO signaling is required for disuse muscle atrophy and is directly regulated by Hsp70. *Am. J. Physiol. Cell Physiol.* 298: C38–45, 2010.

88. **Seoane J, Le H-V, Shen L, Anderson S a, Massagué J**. Integration of Smad and forkhead pathways in the control of neuroepithelial and glioblastoma cell proliferation. *Cell* 117: 211–23, 2004.

89. **Seoane J, Le H-V, Shen L, Anderson S a, Massagué J**. Integration of Smad and forkhead pathways in the control of neuroepithelial and glioblastoma cell proliferation. *Cell* 117: 211–23, 2004.

90. **Shi Y, Wang YF, Jayaraman L, Yang H, Massagué J, Pavletich NP**. Crystal structure of a Smad MH1 domain bound to DNA: insights on DNA binding in TGF-beta signaling. *Cell* 94: 585–94, 1998..

91. **Sishi B, Loos B, Ellis B, Smith W, du Toit EF, Engelbrecht A-M**. Diet-induced obesity alters signalling pathways and induces atrophy and apoptosis in skeletal muscle in a prediabetic rat model. *Exp. Physiol.* 96: 179–93, 2011.

92. **Sitnick M, Bodine SC, Rutledge JC**. Chronic high fat feeding attenuates load-induced hypertrophy in mice. *J. Physiol.* 587: 5753–5765, 2009.

93. **Stitt TN, Drujan D, Clarke BA, Panaro F, Timofeyva Y, Kline WO, Gonzalez M, Yancopoulos GD, Glass DJ, Pharmaceuticals R, York N**. The IGF-1 / PI3K / Akt Pathway Prevents Expression of Muscle Atrophy-Induced Ubiquitin Ligases by Inhibiting FOXO Transcription Factors. *Mol. Cell* 14: 395–403, 2004.

94. **Sun X, Yu Y, Han L**. High FFA levels related to microalbuminuria and uncoupling of VEGF-NO axis in obese rats. *Int. Urol. Nephrol.* 45: 1197–207, 2013.

95. **Szulc P, Munoz F, Marchand F, Chapurlat R, Delmas PD**. Rapid loss of appendicular skeletal muscle mass is associated with higher all-cause mortality in older men: the prospective MINOS study. *Am. J. Clin. Nutr.* 91: 1227–36, 2010.

96. **Tan CK, Leuenberger N, Tan MJ, Yan YW, Chen Y, Kambadur R, Wahli W, Tan NS**. Smad3 deficiency in mice protects against insulin resistance and obesity induced by a high-fat diet. *Diabetes* 60: 464–76, 2011.

97. **Tang ED, Nuñez G, Barr FG, Guan KL**. Negative regulation of the forkhead transcription factor FKHR by Akt. *J. Biol. Chem.* 274: 16741–6, 1999.

98. **Tanida I, Minematsu-Ikeguchi N, Ueno T, Kominami E**. Lysosomal turnover, but not a cellular level, of endogenous LC3 is a marker for autophagy. *Autophagy* 1: 84–91, 2005.

99. **Trendelenburg AU, Meyer A, Rohner D, Boyle J, Hatakeyama S, Glass DJ**. Myostatin reduces Akt/TORC1/p70S6K signaling, inhibiting myoblast differentiation and myotube size. *Am. J. Physiol. Cell Physiol.* 296: C1258–70, 2009.

100. **Waddell DS, Baehr LM, van den Brandt J, Johnsen S a, Reichardt HM, Furlow JD, Bodine SC**. The glucocorticoid receptor and FOXO1 synergistically activate the skeletal muscle atrophy-associated MuRF1 gene. *Am. J. Physiol. Endocrinol. Metab.* 295: E785–97, 2008.

101. **Watts R, McAinch AJ, Dixon JB, O'Brien PE, Cameron-Smith D**. Increased Smad signaling and reduced MRF expression in skeletal muscle from obese subjects. *Obesity.* 21: 525–8, 2013.

102. **Wehling M, Cai B, Tidball JG**. Modulation of myostatin expression during modified muscle use. *FASEB J.* 14: 103–10, 2000.

103. **Welle S, Nair KS**. Relationship of resting metabolic rate to body composition and protein turnover. *Am. J. Physiol.* 258: E990–8, 1990.

104. **Wilkinson KD**. Ubiquitination and deubiquitination: targeting of proteins for degradation by the proteasome. *Semin. Cell Dev. Biol.* 11: 141–8, 2000.

105. **Wing SS**. Deubiquitinases in skeletal muscle atrophy. *Int. J. Biochem. Cell Biol.* 45: 2130–5, 2013.

106. **Wu JJ, Quijano C, Chen E, Liu H, Cao L, Fergusson MM, Rovira II, Gutkind S, Daniels MP, Komatsu M, Finkel T**. Mitochondrial dysfunction and oxidative stress mediate the physiological impairment induced by the disruption of autophagy. *Aging.* 1: 425–37, 2009.

107. **Zhao J, Brault JJ, Schild A, Cao P, Sandri M, Schiaffino S, Lecker SH, Goldberg AL**. FoxO3 coordinately activates protein degradation by the autophagic/lysosomal and proteasomal pathways in atrophying muscle cells. *Cell Metab.* 6: 472–83, 2007.

108. **Zhu X, Topouzis S, Liang L-F, Stotish RL**. Myostatin signaling through Smad2, Smad3 and Smad4 is regulated by the inhibitory Smad7 by a negative feedback mechanism. *Cytokine* 26: 262–72, 2004.

# Appendix A: Institutional review board approval

EAST CAROLINA UNIVERSITY
University & Medical Center Institutional Review Board Office
1L-09 Brody Medical Sciences Building: Mail Stop 682
600 Moye Boulevard Greenville, NC 27834
Office 252-744-2914 · Fax 252-744-2284 · www.ecu.edu/irb

## Notification of Continuing Review Approval

From: Biomedical IRB
To: Jose O. Maldonado
CC:

Gabriel Dubin
Date: 12/21/2011
Re: CRC0000118
UMCIRB 06-0080
Lipid Metabolism in Obesity, Weight Loss and Exercise (2): Muscle Cell Studies

I am pleased to inform you that at the convened meeting on 12/21/2011 12:00 AM of the Biomedical IRB, this research study underwent a continuing review and the committee voted to approve the study. Approval of the study and the consent form(s) is for the period of 12/21/2011 to 12/20/2012.

The Biomedical IRB deemed this study Greater than Minimal Risk.

Ongoing IRB approval research may not be initiated without UMCIRB review except when necessary to eliminate an apparent immediate hazard to the participant. All unanticipated problems involving risks to participants and others must be promptly reported to the UMCIRB. The investigator must submit a continuing review/closure application to the UMCIRB prior to the date of study expiration. The investigator must adhere to all reporting requirements for this study.

The approval includes the following items:

| Name | Description | Modified | Version |
|---|---|---|---|
| Advertisement.fb | Recruitment Documents/Scripts | 12/6/2011 7:48 PM | 0.01 |
| Full Protocol | Study Protocol or Grant Application | 12/8/2011 7:36 PM | 0.01 |
| Protocol | Study Protocol or Grant Application | 12/8/2011 7:18 PM | 0.01 |
| Version 4 exercise training.doc | Consent Forms | 12/8/2011 8:28 PM | 0.01 |
| Version 4 cell culture studies.doc | Consent Forms | 12/8/2011 8:27 PM | 0.01 |
| Version 4 HFD and exercise.doc | Consent Forms | 12/8/2011 8:28 PM | 0.01 |
| Version 4 HFD and weight loss.doc | Consent Forms | 12/8/2011 8:28 PM | 0.01 |
| Version 4 HFD.doc | Consent Forms | 12/8/2011 8:28 PM | 0.01 |

The following UMCIRB members were recused for reasons of potential for Conflict of Interest on this research study: